(Multiskan JX, Thermo Labsystems, Helsinki). Experiments were performed in triplicate.

Statistical analysis. All data were expressed as means ± SE. The significance of differences between group means was analyzed by ANOVA followed by Bonferroni test for samples. Values of $p < 0.05$ were considered statistically significant.

Results

Expression of BTG1 mRNA was down-regulated during proliferation in endothelial cells

To examine whether expression of BTG1 is regulated during cell proliferation in vascular endothelial cells, two types of cultured endothelial cells, HUVECs or BAECs, were used in this study. HUVECs were stimulated with 20% serum following growth-arrest with 0.5% FBS for 48 h. BAECs were stimulated with 10% serum following serum-starvation for 48 h. Total RNA was isolated from these cells at various time points and Northern blot analysis was performed to evaluate the expression level of BTG1 mRNA. As depicted in Figs. 1A and B, the highest expression of BTG1 mRNA was detected in unstimulated (quiescent) endothelial cells. Addition of serum to the cells resulted in time-dependent decreases of BTG1 mRNA levels. At 12–24 h of serum stimulation, the expression level decreased to 38% and 23% of the basal level in HUVEC and BAEC, respectively. When cells reached confluency at ~48 h, the expression of BTG1 mRNA increased, returning to the basal level, probably due to contact inhibition of cell proliferation (Figs. 1A and B).

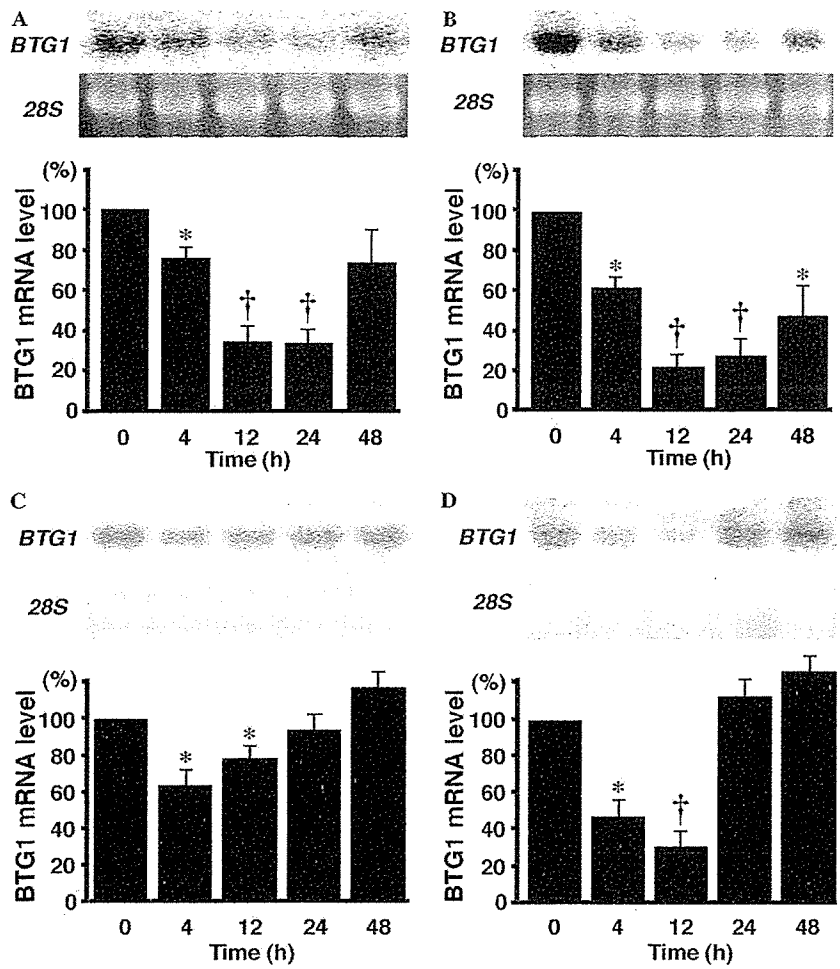

Fig. 1. Down-regulation of BTG1 mRNA by serum or growth factors in endothelial cells. (A) Quiescent HUVECs, growth-arrested in 0.5% FBS for 48 h, were stimulated with 20% serum. (B) Quiescent BAECs, growth-arrested by serum starvation for 48 h, were stimulated with 10% serum. (C) Quiescent HUVECs, growth-arrested in 0.5% FBS for 48 h, were stimulated with VEGF (50 ng/mL). (D) Quiescent BAECs, growth-arrested by serum starvation for 48 h, were stimulated with bFGF (10 ng/mL). Total RNAs were extracted at the indicated time points and subjected to Northern blot analysis. Representative results are shown in the top panels. The ribosomal 28S RNA is shown in the middle panels. Expression levels were quantitated and compared to basal expression in the bottom panels. $^{*}p < 0.05$, $^{\dagger}p < 0.01$ vs. basal expression level ($n = 5$).

We next examined the effect of angiogenic growth factors on BTG1 mRNA levels. Expression of BTG1 mRNA was abundant in growth-arrested HUVECs or BAECs. However, the BTG1 mRNA level was down-regulated by stimulation with VEGF (50 ng/mL) and bFGF (10 ng/mL). At 4–12 h BTG1 mRNA levels were decreased to 64% of the basal level by VEGF in HUVEC and to 34% by bFGF in BAEC (Figs. 1C and D). When cells grow and reach confluency at 24–48 h, BTG1 mRNA was increased and returned to basal level, due to the contact inhibition of cell proliferation (Figs. 1C and D). These findings indicate that BTG1 mRNA expression was down-regulated during proliferation in vascular endothelial cells, and that expression level of BTG1 mRNA was directly related to the proliferation of endothelial cells.

BTG1 mRNA expression was up-regulated in tube-forming endothelial cells

To clarify if BTG1 mRNA expression was regulated in endothelial cells undergoing tube-like network formation, we employed an in vitro angiogenesis assay. HUVECs were plated on Matrigel for induction of tube formation and total RNA was isolated for Northern blot analysis. As shown in Fig. 2A, BTG1 mRNA expression was increased by 3-fold at 3 h after plating on Matrigel, and the up-regulation continued from 3 to 12 h (Fig. 2A). The tube formation of endothelial cells was observed at 2 h and completed within 12 h (data not shown), indicating that up-regulation of BTG1 was concomitant with the tube-like formation of endothelial cells.

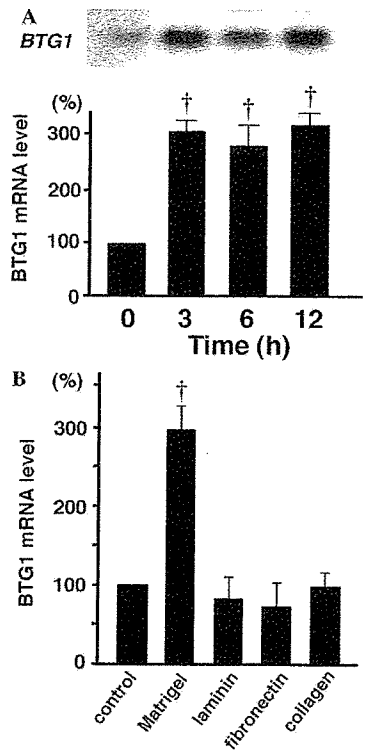

Fig. 2. Up-regulation of BTG1 mRNA expression during in vitro tube formation. (A) HUVECs were plated on the 6-well culture plates coated with Matrigel (1.5×10^5/well) and total RNAs were extracted at the indicated time points. BTG1 mRNA levels were analyzed by Northern blotting. (B) HUVECs were plated on culture plates coated with Matrigel, laminin, fibronectin, collagen, or vehicle (control). BTG1 mRNA levels were compared to the basal level. $^{\dagger}p < 0.01$ vs. basal expression level ($n = 5$).

Matrigel is a basement membrane matrix derived from mouse sarcoma and contains a variety of growth factors and ECMs [16,17]. Because the adhesion of endothelial cells to ECMs induces phenotypic changes mainly through integrin signaling and consequently regulates cell growth or apoptosis, we examined if interaction of endothelial cells with ECMs can affect BTG1 expression. HUVECs were plated on culture dishes coated with Matrigel, fibronectin, laminin or collagen, and BTG1 mRNA expression was evaluated by Northern blotting. Although there was an increase in BTG1 mRNA in HUVECs grown on Matrigel-coated dishes, only minimal changes were observed in HUVECs plated on dishes coated with laminin, fibronectin or collagen (Fig. 2B). The findings suggest that interaction of endothelial cells with ECMs does not primarily regulate BTG1 expression in tube forming endothelial cells on Matrigel.

Among the growth factors contained in the Matrigel, TGF-β is thought to have an essential role in maturation of vascular structures, including interaction between endothelial cells and smooth muscle cells or pericytes [18–20]. Therefore, we examined the effect of TGF-β on BTG1 mRNA expression in endothelial cells. Northern blot analysis revealed a rapid and transient increase in BTG1 mRNA expression by TGF-β (1 ng/mL) after 2 h in BAECs (Fig. 3A), suggesting that activation of the TGF-β pathway plays some role in the process.

To confirm the involvement of TGF-β, we next tested whether neutralizing antibodies against TGF-β could inhibit up-regulation of BTG1 mRNA expression on Matrigel. As shown in Fig. 3B, BTG1 mRNA expression was up-regulated at 3 h after plating on Matrigel. Interestingly, the up-regulation of BTG1 was inhibited by approximately 55% by addition of anti-TGF-β neutralizing antibody ($p < 0.05$ vs. vehicle). These results suggest that up-regulation of BTG1 in tube-forming endothelial cells is evoked, at least in part, by activation of TGF-β signaling pathway.

Gene transfer of sense or antisense BTG1 modulates in vitro angiogenesis

Expression analysis showed that BTG1 mRNA was up-regulated in tube-forming endothelial cells on

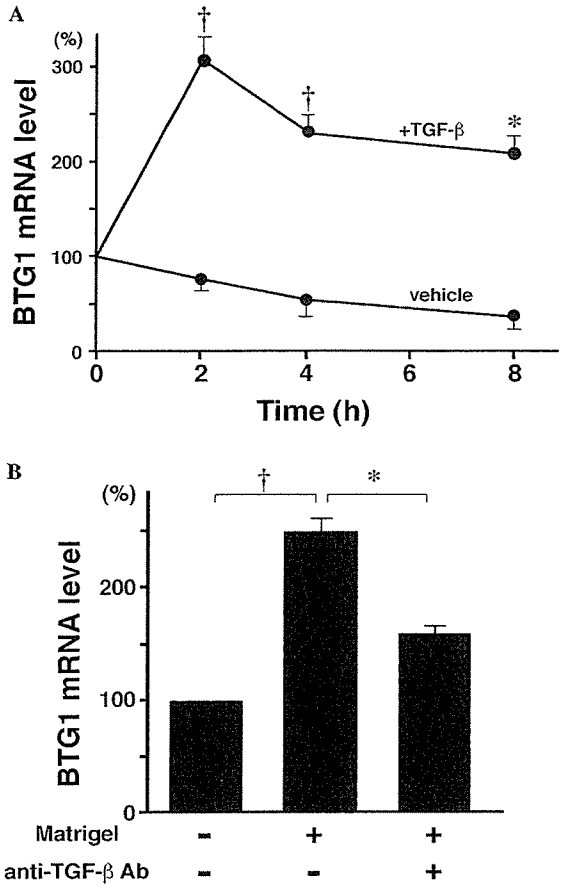

Fig. 3. Up-regulation of BTG1 by TGF-β in BAEC. (A) Pre-confluent BAECs were stimulated with TGF-β (1 ng/mL). Total RNAs were extracted at the indicated times after stimulation. The graph shows that TGF-β caused a rapid increase in BTG1 mRNA levels. (B) HUVECs were plated onto the surface of the Matrigel containing anti-TGF-β neutralizing antibody (anti-TGF-β Ab) or vehicle was dispensed into 6-well tissue culture dishes. The graph shows that the increase in BTG1 mRNA level on Matrigel was blocked by anti-TGF-β Ab. $^{*}p < 0.05$, $^{\dagger}p < 0.01$ vs. basal expression level ($n = 5$).

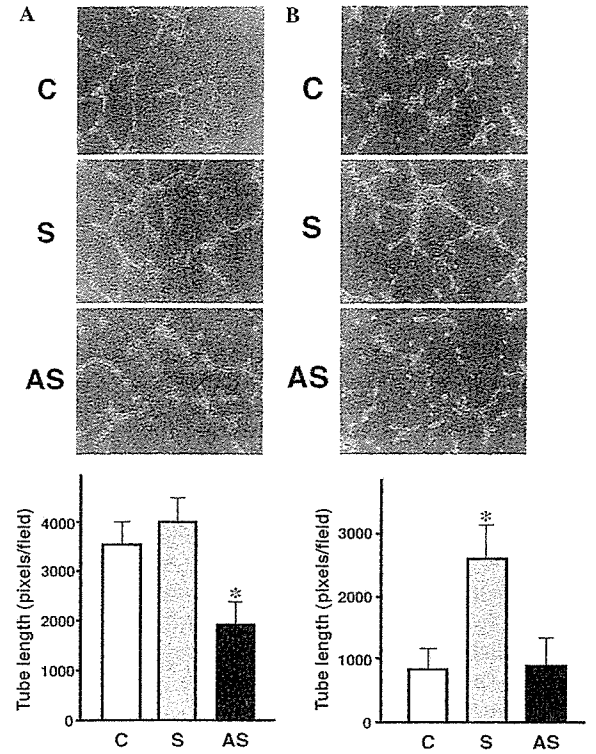

Fig. 4. Gene transfer of sense or antisense BTG1 modulates in vitro network formation. (A) Transfection of antisense BTG1 in EA.hy926 cells attenuated tube formation on Matrigel. (B) Overexpression of sense BTG1 in EA.hy926 cells accelerated tube formation of EA.hy926 cells on growth factor-reduced Matrigel. Matrigel or Growth factor-reduced Matrigel was dispensed into 24-well culture plates. Control (C), sense (S)-, and antisense (AS)-BTG1 transfected EA.hy926 were plated at the density of 4×10^4/well. The total network length per each field was measured and compared among the clones. $^{*}p < 0.05$ vs. basal expression level ($n = 5$).

Matrigel, and that TGF-β is likely involved in this up-regulation of BTG1 on Matrigel. We therefore hypothesized that BTG1 has effects on phenotypic changes of endothelial cells during such processes as tube formation. To test this hypothesis, human vascular endothelial cell lines (EA.hy926), which stably expresses sense or antisense BTG1 cDNA, were generated. These cells were plated on Matrigel, and tube formation was compared with control (pcDNA3 vector-transfected) EA.hy926 cells. Control EA.hy926 cells underwent morphological rearrangements similar to HUVEC when seeded on Matrigel. No significant differences in tube length were detected between control and sense BTG1-overexpressing EA.hy926 cells. However, network formation on Matrigel was markedly attenuated in EA.hy926 cells transfected with antisense BTG1 compared to control cells (Fig. 4A). Most of antisense BTG1-transfected cells aggregated and formed clusters while control cells showed morphological changes such as elongation and lining that are accompanied by network formation (Fig. 4A). The identical result was obtained with all four independent clones examined.

To evaluate the effect of BTG1 on tube-formation in only limited angiogenic cytokines, in vitro tube formation assays were performed using growth factor reduced Matrigel, in which concentrations of growth factors and cytokines were lower than those in regular Matrigel. When cells were plated on growth factor-reduced Matrigel, tube-like formations were significantly increased in EA.hy926 cells stably overexpressing sense BTG1, compared to control cells (Fig. 4B). In contrast, network formation was not affected in antisense-transfected cells (Fig. 4B). The finding indicates that, when angiogenic processes highly stimulated by cytokines abundantly exist in the Matrigel, decreased BTG1 expression resulted in attenuated tube formation. On the other hand,

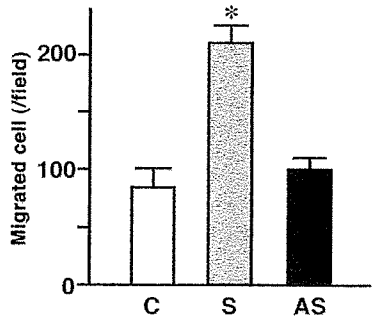

Fig. 5. BTG1 regulates endothelial cell migration. Overexpression of sense BTG1 promoted migration of the EA.hy926 cell. Control (C), sense (S)-, and antisense (AS)-BTG1 transfected clones were evaluated using a modified Boyden chamber system. $^*p < 0.05$ vs. basal expression level ($n = 5$).

on the growth factor-reduced Matrigel, where only minimum angiogenic stimuli exist, up-regulation of BTG1 resulted in accelerated tube formation. Thus, the data implicate that BTG1 mediates intracellular signals in endothelial differentiation, and subsequently regulates cytoskeletal changes in endothelial cells and tube formation.

BTG1 promotes endothelial cell migration

We examined the role of BTG1 in endothelial cell migration. Chemokinesis of sense-transfected, antisense-transfected, and control EA.hy926 cells was evaluated using a modified Boyden chamber system. Migration of sense BTG1-overexpressing clone was significantly increased when compared to control cells in response to 5% serum (Fig. 5). However, there was no difference in cell migration between control and antisense BTG1-transfected EA.hy926 cells. Our results indicate that BTG1 positively regulates migratory activities of vascular endothelial cells. We have finally investigated if BTG1 regulates cell adhesion to ECM such as fibronectin, collagen, and laminin. However, there was no significant difference in cell adhesion to extracellular matrix among sense, antisense and control clones (data not shown).

Discussion

In our previous study, we sought to characterize genes that are regulated in tube-forming HUVECs on Matrigel by PCR-based subtraction cloning in order to identify novel candidate genes for angiogenesis [21,22]. BTG1 was found to be one of the genes up-regulated in tube-forming endothelial cells on Matrigel, and thus we have hypothesized that BTG1 plays a role in endothelial cell biology. To validate this hypothesis, in the present study, we have investigated the regulation of BTG1 mRNA expression and the functional roles of BTG1 in cultured vascular endothelial cells. We have demonstrated here for the first time that BTG1 is highly expressed in the quiescent vascular endothelial cells and the expression is decreased in the proliferating endothelial cells stimulated with serum or growth factors such as VEGF and bFGF. The regulated expression of this gene during the cell proliferation is consistent with the reported observation in other cell types. These results suggest that BTG1 may regulate endothelial cell proliferation.

In the present experiments, BTG1 was up-regulated in the tube-forming endothelial cells on Matrigel. Matrigel has been well recognized and used for in vitro model of angiogenesis. Matrigel contains a variety of extracellular matrices as well as angiogenic growth factors. Vascular endothelial cells make network formation with tube-like structure when seeded on Matrigel. The in vitro capillary network formation on Matrigel, in general, requires endothelial cells to stop proliferation, and in turn to differentiate and migrate into tube-like network formation [23,24]. The up-regulation of BTG1 mRNA by Matrigel was partially blocked by anti-TGF-β antibody. In contrast to VEGF and bFGF, TGF-β itself increased mRNA expression of BTG1 in HUVECs. TGF-β is one of the most important regulators for endothelial cell proliferation and promotes cell differentiation [25]. Considering the potential action of TGF-β on endothelial cell growth, it is assumed that TGF-β modulates tube formation at least in part by activation of BTG1 in vascular endothelial cells.

The regulated expression of BTG1 during endothelial cell proliferation and tube-formation suggested that BTG1 may contribute to the process of angiogenesis through the modulation of endothelial functions. To confirm if the regulated expression of BTG1 is functionally relevant in in vitro angiogenic processes, we modulated BTG1 levels in endothelial cells by transfection of sense or antisense BTG1 cDNA. Interestingly, transfection studies have documented that modulation of BTG1 level in endothelial cells was directly related to the degree of tube formation. Forced overexpression of BTG1 in the endothelial cell line by sense gene transfer resulted in accelerated tube formation, and down-regulation by antisense gene transfer resulted in inhibited tube formation in this in vitro model of angiogenesis. In addition, BTG1 overexpression significantly promoted cell migration in the sense BTG1 transfected cells. The findings suggest that up-regulation of BTG1 is functionally relevant in endothelial phenotypic changes. Taken together, we speculate that BTG1 may regulate cell cycle and phenotype in endothelial cells, and consequently modulate formation and maintenance of blood vessels.

It has been implicated that the function of BTG1 is achieved by interaction with different cellular targets.

BTG1 has been shown to interact with PRMT1 (protein arginine methyltransferase of type 1), an arginine *N*-methyltransferase that plays an important role in the anti-proliferative function, and modulate its activity positively in non-endothelial cells [26]. BTG1 can also interact with Caf1, a component of the CCR4 complex, which regulates the expression of a number of genes involved in cell cycle regulation and progression [27–29]. In neuronal cells, BTG1 interacts with HoxB9 to enhance the transcription of an immunoglobulin family adhesion molecule NCAM, involved in the neurogenesis. The molecular mechanisms underlying BTG1's regulation of angiogenesis remain unclear in endothelial cells. Further studies are required to clarify the intracellular mechanism for BTG1 actions in the endothelial cells.

In conclusion, the anti-proliferative gene BTG1 is expressed by quiescent vascular endothelial cells and down-regulated during the cell growth. Besides the anti-proliferative action, BTG1 promotes cell migration and plays a role in angiogenesis. Accordingly, modulation of BTG1 pathway is a novel target for control of blood vessel formation in physiological and pathological angiogenesis.

References

[1] W. Risau, Mechanisms of angiogenesis, Nature 386 (1997) 671–674.

[2] J. Folkman, Angiogenesis in cancer, vascular, rheumatoid and other disease, Nat. Med. 1 (1995) 27–31.

[3] N. Boudreau, C. Andrews, A. Srebrow, A. Ravanpay, D.A. Cheresh, Induction of the angiogenic phenotype by Hox D3, J. Cell Biol. 139 (1997) 257–264.

[4] C. Myers, A. Charboneau, N. Boudreau, Homeobox B3 promotes capillary morphogenesis and angiogenesis, J. Cell Biol. 148 (2000) 343–351.

[5] R. Rimokh, J.P. Rouault, K. Wahbi, M. Gadoux, M. Lafage, E. Archimbaud, C. Charrin, O. Gentilhomme, D. Germain, J. Samarut, et al., A chromosome 12 coding region is juxtaposed to the MYC protooncogene locus in a t(8;12)(q24;q22) translocation in a case of B-cell chronic lymphocytic leukemia, Genes Chromosomes Cancer 3 (1991) 24–36.

[6] J.P. Rouault, R. Rimokh, C. Tessa, G. Paranhos, M. Ffrench, L. Duret, M. Garoccio, D. Germain, J. Samarut, J.P. Magaud, BTG1, a member of a new family of antiproliferative genes, EMBO J. 11 (1992) 1663–1670.

[7] S. Matsuda, J. Rouault, J. Magaud, C. Berthet, In search of a function for the TIS21/PC3/BTG1/TOB family, FEBS Lett. 497 (2001) 67–72.

[8] M.H. Corjay, M.A. Kearney, D.A. Munzer, S.M. Diamond, J.K. Stoltenborg, Antiproliferative gene BTG1 is highly expressed in apoptotic cells in macrophage-rich areas of advanced lesions in Watanabe heritable hyperlipidemic rabbit and human, Lab. Invest. 78 (1998) 847–858.

[9] D.J. Raburn, K.G. Hamil, J.K. Tsuruta, D.A. O'Brien, S.H. Hall, Stage-specific expression of B cell translocation gene 1 in rat testis, Endocrinology 136 (1995) 5769–5777.

[10] G.T. Chang, L.J. Blok, M. Steenbeek, J. Veldscholte, W.M. van Weerden, G.J. van Steenbrugge, A.O. Brinkmann, Differentially expressed genes in androgen-dependent and -independent prostate carcinomas, Cancer Res. 57 (1997) 4075–4081.

[11] A. Rodier, S. Marchal-Victorion, P. Rochard, F. Casas, I. Cassar-Malek, J.P. Rouault, J.P. Magaud, D.Y. Mason, C. Wrutniak, G. Cabello, BTG1: a triiodothyronine target involved in the myogenic influence of the hormone, Exp. Cell Res. 249 (1999) 337–348.

[12] T. Sakaguchi, A. Kuroiwa, H. Takeda, Expression of zebrafish btg-b, an anti-proliferative cofactor, during early embryogenesis, Mech. Dev. 104 (2001) 113–115.

[13] S. Marchal, I. Cassar-Malek, J.P. Magaud, J.P. Rouault, C. Wrutniak, G. Cabello, Stimulation of avian myoblast differentiation by triiodothyronine: possible involvement of the cAMP pathway, Exp. Cell Res. 220 (1995) 1–10.

[14] S. Tang, Y. Gao, J.A. Ware, Enhancement of endothelial cell migration and in vitro tube formation by TAP20, a novel beta 5 integrin-modulating, PKC theta-dependent protein, J. Cell Biol. 147 (1999) 1073–1084.

[15] B.M. Glaser, P.A. D'Amore, H. Seppa, S. Seppa, E. Schiffmann, Adult tissues contain chemoattractants for vascular endothelial cells, Nature 288 (1980) 483–484.

[16] P.G. McGuire, N.W. Seeds, The interaction of plasminogen activator with a reconstituted basement membrane matrix and extracellular macromolecules produced by cultured epithelial cells, J. Cell Biochem. 40 (1989) 215–227.

[17] H.K. Kleinman, M.L. McGarvey, L.A. Liotta, P.G. Robey, K. Tryggvason, G.R. Martin, Isolation and characterization of type IV procollagen, laminin, and heparan sulfate proteoglycan from the EHS sarcoma, Biochemistry 21 (1982) 6188–6193.

[18] R. Flaumenhaft, M. Abe, Y. Sato, K. Miyazono, J. Harpel, C.H. Heldin, D.B. Rifkin, Role of the latent TGF-beta binding protein in the activation of latent TGF-beta by co-cultures of endothelial and smooth muscle cells, J. Cell Biol. 120 (1993) 995–1002.

[19] Y. Sato, F. Okada, M. Abe, T. Seguchi, M. Kuwano, S. Sato, A. Furuya, N. Hanai, T. Tamaoki, The mechanism for the activation of latent TGF-beta during co-culture of endothelial cells and smooth muscle cells: cell-type specific targeting of latent TGF-beta to smooth muscle cells, J. Cell Biol. 123 (1993) 1249–1254.

[20] J.R. Gamble, S. Bradley, L. Noack, M.A. Vadas, TGF-beta and endothelial cells inhibit VCAM-1 expression on human vascular smooth muscle cells, Arterioscler. Thromb. Vasc. Biol. 15 (1995) 949–955.

[21] K. Hirata, H.L. Dichek, J.A. Cioffi, S.Y. Choi, N.J. Leeper, L. Quintana, G.S. Kronmal, A.D. Cooper, T. Quertermous, Cloning of a unique lipase from endothelial cells extends the lipase gene family, J. Biol. Chem. 274 (1999) 14170–14175.

[22] K. Hirata, T. Ishida, K. Penta, M. Rezaee, E. Yang, J. Wohlgemuth, T. Quertermous, Cloning of an immunoglobulin family adhesion molecule selectively expressed by endothelial cells, J. Biol. Chem. 276 (2001) 16223–16231.

[23] J.R. Merwin, W. Newman, L.D. Beall, A. Tucker, J. Madri, Vascular cells respond differentially to transforming growth factors beta 1 and beta 2 in vitro, Am. J. Pathol. 138 (1991) 37–51.

[24] A.B. Roberts, M.B. Sporn, R.K. Assoian, J.M. Smith, N.S. Roche, L.M. Wakefield, U.I. Heine, L.A. Liotta, V. Falanga, J.H. Kehrl, et al., Transforming growth factor type beta: rapid induction of fibrosis and angiogenesis in vivo and stimulation of collagen formation in vitro, Proc. Natl. Acad. Sci. USA 83 (1986) 4167–4171.

[25] J. Massague, The transforming growth factor-beta family, Annu. Rev. Cell Biol. 6 (1990) 597–641.

[26] W.J. Lin, J.D. Gary, M.C. Yang, S. Clarke, H.R. Herschman, The mammalian immediate-early TIS21 protein and the leukemia-associated BTG1 protein interact with a protein-arginine *N*-methyltransferase, J. Biol. Chem. 271 (1996) 15034–15044.

[27] D. Prevot, A.P. Morel, T. Voeltzel, M.C. Rostan, R. Rimokh, J.P. Magaud, L. Corbo, Relationships of the antiproliferative proteins BTG1 and BTG2 with CAF1, the human homolog of a component of the yeast CCR4 transcriptional complex: involvement in estrogen receptor alpha signaling pathway, J. Biol. Chem. 276 (2001) 9640–9648.

[28] J.P. Rouault, D. Prevot, C. Berthet, A.M. Birot, M. Billaud, J.P. Magaud, L. Corbo, Interaction of BTG1 and p53-regulated BTG2 gene products with mCaf1 the murine homolog of a component of the yeast CCR4 transcriptional regulatory complex, J. Biol. Chem. 273 (1998) 22563–22569.

[29] J.A. Bogdan, C. Adams-Burton, D.L. Pedicord, D.A. Sukovich, P.A. Benfield, M.H. Corjay, J.K. Stoltenborg, I.B. Dicker, Human carbon catabolite repressor protein (CCR4)-associative factor 1: cloning, expression and characterization of its interaction with the B-cell translocation protein BTG1, Biochem. J. 336 (Pt 2) (1998) 471–481.

ELSEVIER

Atherosclerosis 172 (2004) 21–29

ATHEROSCLEROSIS

www.elsevier.com/locate/atherosclerosis

Intramuscular gene transfer of interleukin-10 cDNA reduces atherosclerosis in apolipoprotein E-knockout mice

Masayuki Namiki[a], Seinosuke Kawashima[a,*], Tomoya Yamashita[a], Masanori Ozaki[a], Tsuyoshi Sakoda[a], Nobutaka Inoue[a], Ken-Ichi Hirata[a], Ryuichi Morishita[b], Yasufumi Kaneda[b], Mitsuhiro Yokoyama[a]

[a] *Department of Internal Medicine, Division of Cardiovascular and Respiratory Medicine, Kobe University Graduate School of Medicine, 7-5-2 Kusunoki-cho, Chuo-ku, Kobe 650-0017, Japan*

[b] *Department of Geriatric Medicine, Division of Gene Therapy Science, Graduate School of Medicine, Osaka University, Osaka, Japan*

Received 15 June 2003; received in revised form 21 July 2003; accepted 11 August 2003

Abstract

Atherosclerosis has a close relationship to inflammation, particularly T helper type 1 lymphocyte (Th1) response. Interleukin-10 (IL-10), is thought to suppress Th1 response. To target therapeutic strategy for atherosclerosis, we tested whether IL-10 gene transfer suppresses atherosclerosis in apolipoprotein E-knockout (apoE-KO) mice. Four-week-old apoE-KO mice were divided into two groups and either murine IL-10 cDNA plasmid or empty control vector was transferred to the femoral muscle with the use of Hemagglutinating virus of Japan (HVJ)-liposome. At 1 week after transfection, high cholesterol diet was started and continued for 8 weeks. After euthanasia, histological studies of atherosclerotic lesions and quantitative RT-PCR for Th1 cytokines (IL-12 and IFN-γ) in spleens were performed. IL-10 cDNA gene transfer to the muscle increased plasma IL-10 levels and depressed expression of Th1 cytokines without changing plasma cholesterol levels. IL-10 gene transfer significantly reduced the atherosclerotic plaque area and the macrophage infiltrated area. IL-12 and IFN-γ mRNA expressions in spleens and plasma IFN-γ levels were decreased by IL-10 gene transfer. Therefore, IL-10 gene transfer changed the Th1 response and suppressed atherosclerotic lesion formation in apoE-KO mice. IL-10 could be a new target as a therapeutic tool for the treatment of atherosclerosis.

Keywords: Interleukin-10; Apolipoprotein E-knockout mouse; Atherosclerosis; Gene therapy

1. Introduction

Atherosclerosis is thought to have a close relationship to inflammation throughout the different stages of lesion development [1]. While a large number of evidence exists to support a role of pro-inflammatory cytokines on atherogenesis [2], information regarding the potential role of anti-inflammatory cytokines is limited. During the inflammatory reaction, anti-inflammatory cytokines are also produced and modulate the inflammatory process [3].

Interleukin-10 (IL-10), secreted by T helper type 2 (Th2) lymphocytes and also in large amounts by macrophages, is an anti-inflammatory cytokine with potent deactivating properties on both macrophages and T-lymphocytes [4]. IL-10 blocks the synthesis of macrophage-derived cytokines including IL-1β, IL-12, and tumor necrosis factor-α, and reduces cytotoxic activity of macrophages [5]. IL-10 indirectly reduces T helper type 1 (Th1) lymphocyte differentiation by blocking macrophage IL-12 synthesis [6,7]. Some of the suppressive effects of IL-10 on cytokines and production of inflammatory mediators in tissues may be mediated by inhibition of IFN-γ production [8]. It is reported that daily IL-12 administration caused the acceleration of atherosclerosis, associated with increased serum antibodies to oxidized LDL in apolipoprotein E-knockout (apoE-KO) mice [9]. On the other hand, a number of investigations have shown that IL-10 is involved in the process of atherogenesis [10]. Anti-atherogenic property of IL-10 is demonstrated in vivo studies on diet-induced atherosclerosis in IL-10 deficient mice [11,12]. The protective effects of IL-10 against atherosclerosis might be associated with suppression of Th1 cytokines, particularly IL-12 and IFN-γ.

* Corresponding author. Tel.: +81-78-382-5841; fax: +81-78-382-5859.
E-mail address: kawashim@med.kobe-u.ac.jp (S. Kawashima).

0021-9150/$ – see front matter © 2003 Elsevier Ireland Ltd. All rights reserved.
doi:10.1016/j.atherosclerosis.2003.08.032

In the present study, to target therapeutic strategy for atherosclerosis based on the cytokine modulation, we tested whether IL-10 cDNA gene transfer in the early stage of atherosclerosis could suppress lesion formation in apoE-KO mice. For this purpose, we injected IL-10 cDNA repeatedly into the skeletal muscle using the Hemagglutinating virus of Japan (HVJ)-liposomes method [13,14]. We also examined whether the local IL-10 gene transfer could change the systemic expression of Th1-associated cytokine.

2. Materials and methods

2.1. Plasmid vector

Mouse IL-10 cDNA expression vector (pcDSRalpha-F115) was obtained commercially (American Type Culture Collection, VA). The vector is modified from pcD, with a promoter constructed from the SV40 early promoter and contains the complete coding sequence of mIL-10 [15,16]. The vector pcDSRalpha without expression coding site was used for the control plasmid.

2.2. Preparation of Hemagglutinating virus of Japan-liposome

HVJ-liposomes were prepared as previously described [13]. Briefly, lipids (cholesterol, phosphatidylserine, and phosphatidylcholine) were mixed in a weight ratio of 1:4.8:2. The lipid mixture was placed in the bottom of a glass tube and dried with a rotary evaporator to form a lipid thin layer. The mIL-10 cDNA plasmid (mIL-10-HVJ) or control plasmid HVJ (Cont-HVJ) was incorporated into liposomes by shaking and sonication. The liposomes containing plasmids and HVJ were incubated at 4 °C for 10 min and then at 37 °C for 60 min with gentle shaking to locate the HVJ protein on the surface of the liposomes. These solutions containing HVJ-liposomes were concentrated by a sucrose gradient centrifugation. HVJ-liposomes containing mIL-10 cDNA plasmid or control plasmid were intramusclerly injected into mice in a total volume of 0.1 ml.

2.3. Animal preparation and experimental design

Twenty male apoE-KO mice (offsprings of homozygous apoE-KO mice backcrossed onto the C57BL/6J background) were weaned and divided into two groups at 4 weeks of age. The mIL-10-HVJ or Cont-HVJ was injected to the mouse femoral muscle every 2 weeks for 5 times. The mice in both groups were switched to an atherogenic high-cholesterol diet (normal chow diet containing 1.25% cholesterol, 7.5% cocoa butter, 7.5% casein, and 0.5% sodium cholate, Oriental Yeast, Japan) 1 week after the first HVJ administration. The mice were euthanized a week after the final gene transfer (13 weeks of age). In additional group of apoE-KO mice, changes in plasma levels of IL-10 were measured after single mIL-10-HVJ administration. The mice were provided the diet and water ad libitum and maintained on a 12 h light/dark cycle. All animal experiments were conducted according to the Guidelines for Animal Experiments at Kobe University School of Medicine.

2.4. Plasma lipid and cytokine analyses

After overnight fasting, blood sampling was done by left ventricle puncture on the day of euthanasia. Plasma was separated by centrifugation and stored at −80 °C until the assays. Plasma total cholesterol and triglyceride levels were measured by an automated clinical chemistry analyzer. HDL-cholesterol levels were quantified by enzymatic reaction using a commercially available kit (Wako, Japan). Mouse plasma IL-10 and IFN-γ levels were measured with mouse ELISA kits for each cytokine (Biosourse International, CA).

2.5. Histological analysis of atherosclerotic lesions

The aortic root including myocardium of the left ventriclar outflow was removed, fixed with 10% formaldehyde, equilibrated in 20% sucrose, and embedded in OCT compounds (Tissue-Tek, CA). Cryosections (10 μm thickness) spanning 550 μm of the aortic root were cut and collected. The most proximal site started where the three aortic valve first appeared. Five sections (every tenth section, each 100 μm apart) from the individual mouse were stained with Sudan III, hematoxylin and eosin, and Sirius red. Quantification of atherosclerotic lesion was performed by two observers (M.O. and T.Y.) blinded to the experimental protocol. The total lesion area of five sections from each mouse was measured with the use of NIH Imaging Software according to the method described by Paigen et al. [17].

2.6. Immunohistochemistry

At least three different sections of the aortic root from the individual mice were stained with an anti-mouse monocyte/macrophage monoclonal rat antibody (MOMA-2, Biosource International, CA), an anti-human T-cell polyclonal rabbit antibody (CD3, DAKO A/S, Denmark), a rat monoclonal anti-VCAM-1 antibody (M/K-2, CHEMICON International, CA), and a mouse monoclonal anti-ICAM-1 antibody (KAT-1, Genzyme/Techne, CA). Biotinylated anti-mouse and anti-rabbit secondary antibodies (DAKO A/S) were detected with streptavidin-peroxidase and 3′3′-diaminobenzidine substrate. Quantitative analysis of the positive staining area was performed as described previously, and the percentage of the positive staining area (the positive staining area/total atherosclerotic lesion area × 100) was calculated [18].

2.7. Semiquantitative reverse transcription-polymerase chain reaction

Total RNA from each spleen specimen was isolated with ISOGEN (Nippon Gene, Japan) according to the manufacturer's instruction. Messenger RNAs were reverse transcribed into cDNA with the reverse transcription kit (Ambion Inc, TX). Semiquantitative reverse transcription-polymerase chain reaction (RT-PCR) was carried out on 2 μl of these cDNA solution (RT products) added to the aimed constructed sense and anti-sense primers, commercially available 18S primers set (No.1716, Ambion Inc, TX), 0.2 mmol/l dNTP, PCR buffer (10 mmol/l Tris–HCl, pH 8.3, 50 mmol/l KCl, 0.001% gelatin), and 2.5 U Taq polymerase (Takara, Japan). The primers used for analysis of IL-12p40 were 5′-CAG AAG CTA ACC ATC TCC TGG TTT G-3′ (sense), and 5′-TCC GGA GTA ATT TGG TGC TTC ACA C-3′ (antisense); for IFN-γ, 5′-AGC GGC TGA CTG AAC TCA GAT TG-3′ (sense), and 5′-GTC ACA GTT TTC AGC TGT ATA GG-3′ (antisense), synthesized commercially (Japan Bioservice, Japan) [9]. The reaction proceeded for 30 cycles in a programmable DNA thermal cycler (ASTEC PC-700; ASTEC, Japan), with denaturation at 94 °C for 1 min, annealing at 55 °C for 1 min and extension at 72 °C for 1 min, followed by an extension at 70 °C for 10 min. The PCR products electrophoresed on a 2% agarose gel containing ethidium bromide were visualized under UV light, captured by a CCD video monitor and analyzed by the densitograph software (ATTO, Japan).

2.8. Statistics

Data are presented as means ± S.E.M. An unpaired Student's *t*-test was used to detect significant differences when two groups were compared. Statistical differences among groups were determined by one-way ANOVA with Bonferroni correction.

3. Results

3.1. Plasma lipid profile

Total cholesterol levels increased to approximately 50 mmol/l in both Cont-HVJ-treated and mIL-10-HVJ-treated mice, and there were no differences in the lipid profile between the two groups (Table 1).

3.2. IL-10 expressions in the mIL-10-HVJ-treated mice

Plasma IL-10 was not detected by ELISA in Cont-HVJ-treated mice. However, in mIL-10-HVJ-treated mice, plasma IL-10 levels were markedly increased 1 day after transfection (5.2 ± 1.5 pg/ml) and those were returned to the background levels by 3 days after transfection (Fig. 1).

Table 1
Plasma lipid values

	Total cholesterol	Triglyceride	HDL choresterol
Cont-HVJ	51.8 ± 11.4 (8)	0.43 ± 0.16 (8)	1.32 ± 0.47 (8)
mIL-10-HVJ	48.3 ± 2.8 (10)	0.52 ± 0.019 (10)	1.09 ± 0.36 (10)

Values are in mmol/l and expressed as means ± S.E.M. (numbers of mice). Plasma lipid levels were not significantly different between the two groups fed the atherogenic diet for 9 weeks.

3.3. Histological examinations of atherosclerotic lesions in apoE-KO mice

The aortic sinus atherosclerotic lesion areas of apoE-KO mice were measured using the Sudan III-stained sections (Fig. 2A and B). The mIL-10-HVJ treatment dramatically decreased the atherosclerotic plaque area compared with the Cont-HVJ-treated apoE-KO mice (0.461 ± 0.089 versus 1.187 ± 0.141 mm^2, $P < 0.01$; Fig. 2C). Immunostainings for mouse macrophage (MOMA2) revealed that macrophages were predominant in the atherosclerotic plaques in both Cont-HVJ- and mIL-10-HVJ-treated mice (Fig. 3A and B). The macrophage-infiltrated area was suppressed by mIL-10-HVJ-treatment (0.124 ± 0.024 versus 0.300 ± 0.056 mm^2, $P < 0.01$; Fig. 4A). Because the inhibition of macrophage infiltration was proportionate to the plaque-size inhibition, there was no significant difference in the macrophage/plaque area ratio (27.0±5.2% versus 25.3± 4.7%; Fig. 4C). T-lymphocyte infiltration in the atherosclerotic plaques was also examined by immunostaining for CD3 (Fig. 3C and D). There was no difference in the area of T-lymphocyte infiltration between mIL-10-HVJ-treated mice and Cont-HVJ-treated mice (0.030 ± 0.001 versus 0.041 ± 0.009 mm^2; Fig. 4B), and therefore the percent T-lymphocyte-infiltrated area in the plaque was higher in mIL-10-HVJ-treated mice (6.60 ± 0.91% versus 3.48 ± 0.75%, $P < 0.05$; Fig. 4D). On the other hand, a smooth muscle actin-positive cells in the plaque were few or hardly de-

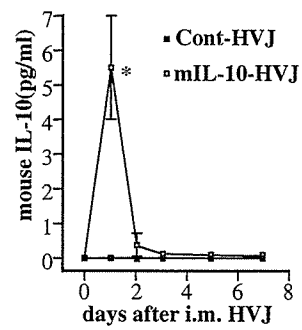

Fig. 1. Plasma IL-10 levels after HVJ injection. Changes in plasma mouse IL-10 levels after transfection of mIL-10-HVJ or Cont-HVJ to the femoral muscle of apoE-KO mice. Values are means ± S.E.M. The number of samples of each spot was at least three. At the basal levels, IL-10 was not detected and Cont-HVJ-treatment did not increase plasma IL-10 levels. However, plasma IL-10 levels were significantly increased on Day 1 ($n = 8$) in mIL10-HVJ-treated mice (*$P < 0.01$).

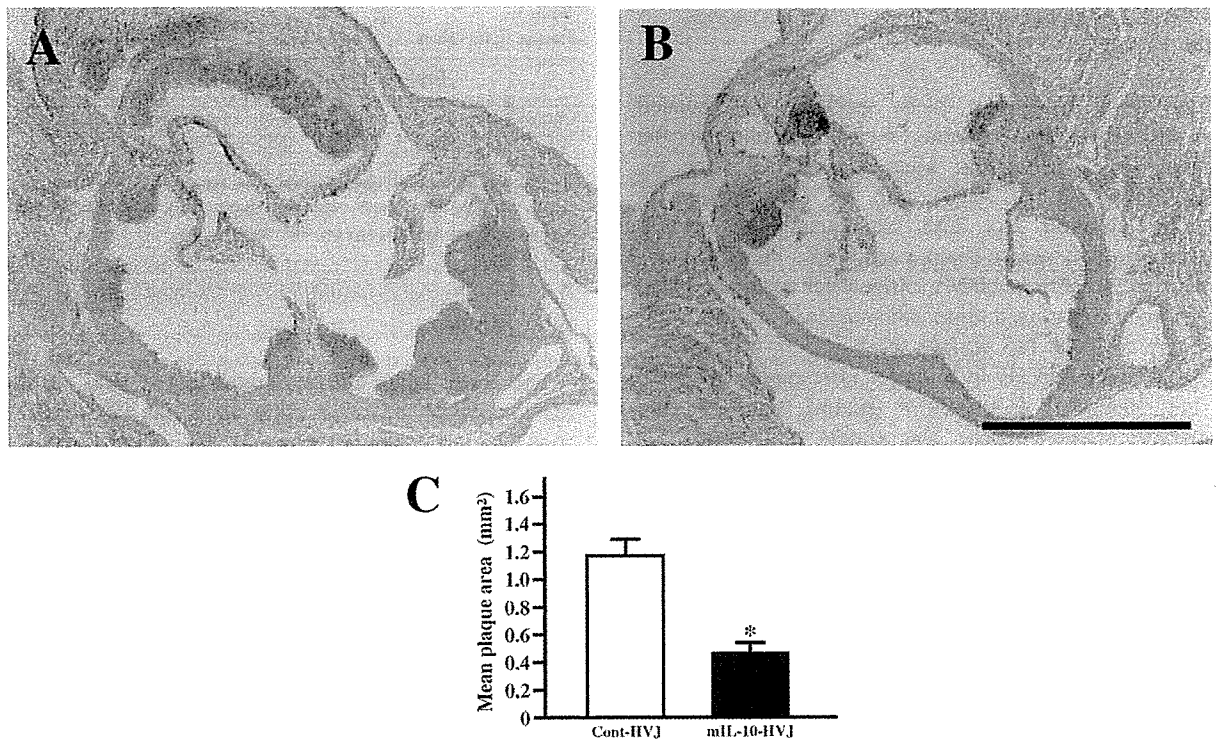

Fig. 2. Atherosclerotic lesions in apoE-KO mice. Sudan III staining, counter stained with hematoxylin, of the aortic sinus from (A) Cont-HVJ- and (B) mIL-10-HVJ-treated mouse, respectively. The mIL-10-HVJ-treatment dramatically decreased the atherosclerotic plaque size compared with the Cont-HVJ treatment. Original magnifications were ×60. A bar indicates 500 μm. (C) Quantitative analysis of atherosclerotic lesion areas in apoE-KO mice. The total lesion area of five sections from each mouse was measured. An open bar indicates the Cont-HVJ-treated group ($n = 8$) and an closed bar shows the mIL-10-HVJ-treated group ($n = 10$). The mIL-10-HVJ treatment dramatically decreased the atherosclerotic plaque area compared with the Cont-HVJ-treated apoE-KO. Values are means ± S.E.M. of each group.

tectable in this early stage of atherosclerotic lesions of both mice (data not shown). Fibrotic changes were only partly distributed in the atherosclerotic lesions and the area stained by Sirius red did not differ between Cont-HVJ-treated and mIL-10-HVJ-treated mice (Fig. 3E and F). In addition, there was no difference in the expression of ICAM-1 or VCAM-1 in either plaque or non-plaque lesion between Cont-HVJ-treated and mIL-10-HVJ-treated mice (Fig. 5).

3.4. Quantitative analysis of IL-12 and IFN-γ mRNA levels in spleens and plasma IFN-γ levels

Expressions of typical Th1-associated cytokine genes in spleens from apoE-KO mice treated with Cont-HVJ or mIL-10-HVJ were analyzed by semiquantitative RT-PCR. Lengths of the amplified fragments were 394 bp for IL-12 and 245 bp for IFN-γ (Fig. 6A). The band-intensity of each cytokine was normalized to 18S transcript (489 bp) as an internal control gene. Treatment with mIL-10-HVJ suppressed the mRNA expressions of IL-12 and IFN-γ in spleens. Both IL-12/18S ratio and IFN-γ/18S ratio were suppressed by 70% in mIL-10-HVJ-treated mice compared with Cont-HVJ-treated mice (Fig. 6B and C). In accordance with the reduced expression of IFN-γ gene in the spleen, plasma IFN-γ levels were decreased in mIL-10-HVJ-treated mice compared with Cont-HVJ-treated mice (5.6 ± 0.9 versus 10.6 ± 1.6 pg/ml, $n = 6$ for each group, $P < 0.05$).

4. Discussion

In this study, we succeeded in reducing atherosclerotic lesion formation by repeated intramuscular IL-10 cDNA injections with the use of HVJ-liposome. Our results are in agreement with previous studies [11,19]. Mallat et al. reported that the atherogenic diet-induced plaque formation was augmented in IL-10-deficient C57BL/6J mice compared with wild-type mice. They also reported that the augmented atherosclerotic lesion size in the IL-10-deficient mice was partially reversed by IL-10 gene transfer to the tibial muscle [11]. Thüsen et al. demonstrated that intravenous adenoviral gene transfer of IL-10 reduced the collar-induced carotid atherosclerosis in low density lipoprotein receptor knockout mice [19]. Our study expanded their findings further in that the repeated IL-10 gene transfer can inhibit atherosclerotic lesion formation in apoE-KO mice, which develop atherosclerotic lesions similar to those seen in humans and are widely used for studying the pathogenesis of

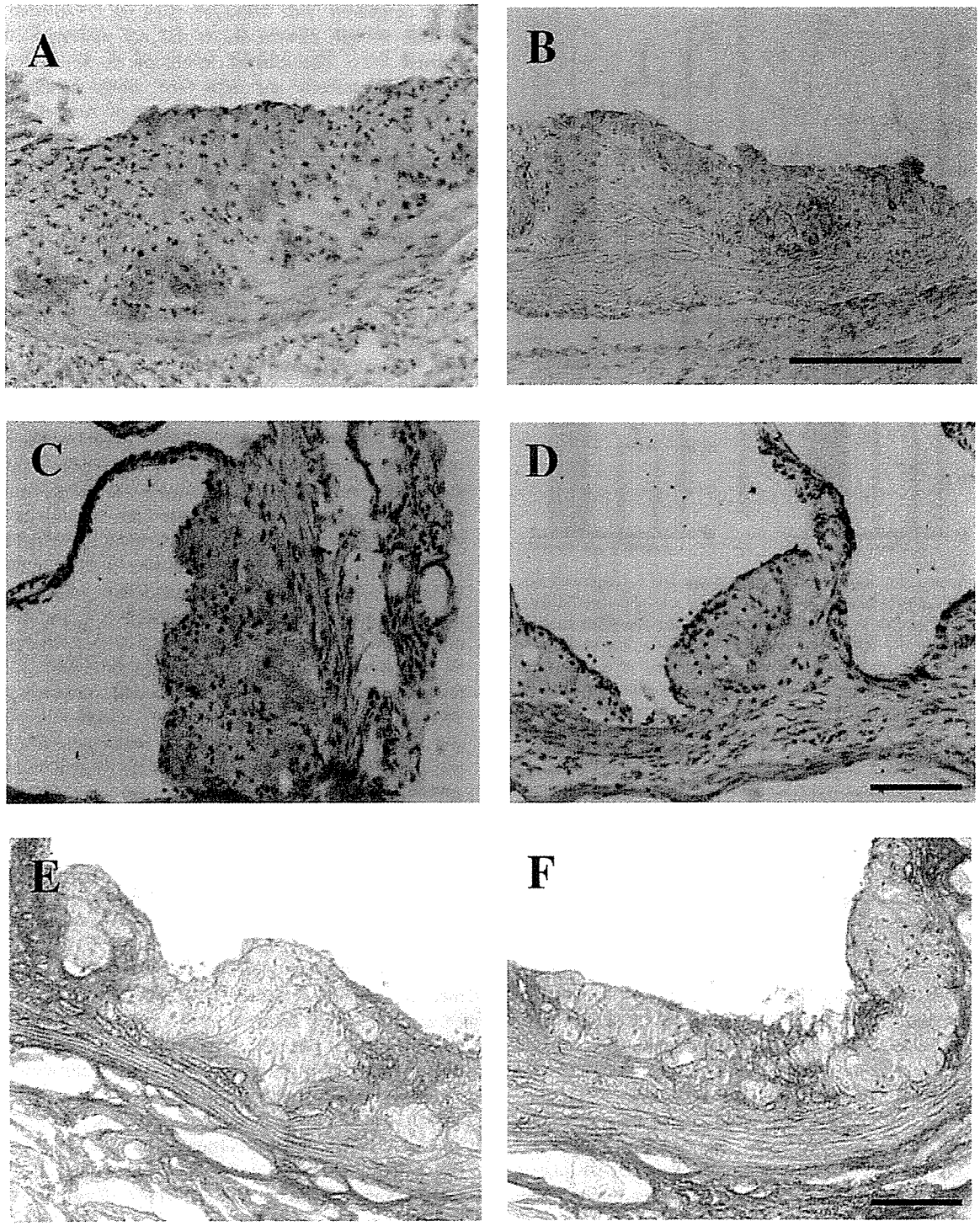

Fig. 3. Characteristics of atherosclerotic lesions in apoE-KO mice. Immunostainings for mouse macrophage (MOMA2) in the atherosclerotic plaque of the aortic sinus from (A) Cont-HVJ- and (B) mIL-10-HVJ-treated mouse, respectively. MOMA2-immunostaining proved diffuse distribution of macrophages in the plaque. Immunostainings for T-lymphocyte (CD3) in the atherosclerotic plaque of the aortic sinus from (C) Cont-HVJ- and (D) mIL-10-HVJ-treated mouse, respectively. The plaque lesions of almost the same lesion size was used for Sirius red staining. There were no differences in the Sirius red-stained areas in the plaque between (E) Cont-HVJ- and (F) mIL-10-HVJ-treated mouse. Original magnifications were A and B; ×200, C, D, E and F; ×100. Bars indicate 100 μm.

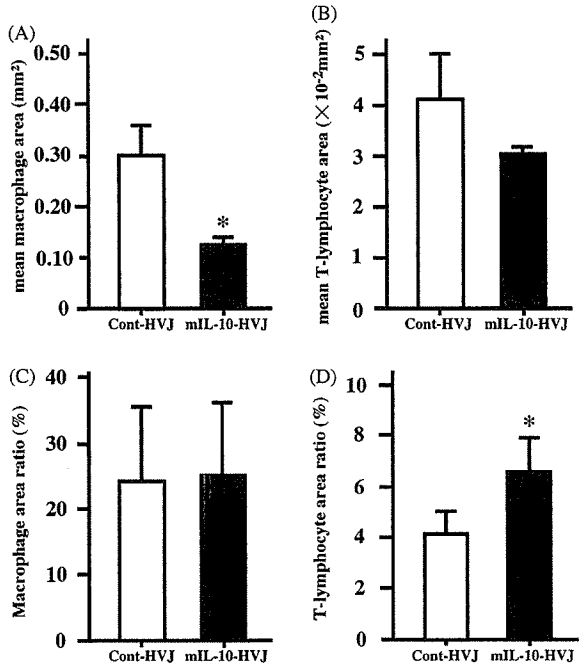

Fig. 4. Quantitative analysis of the macrophage and T-lymphocyte contents in the atherosclerotic plaque. Plaque area and immunohistochemically stained area for macrophages (MOMA2) and T-lymphocytes (CD3) were measured by NIH image software. (A) Mean macrophage and (B) T-lymphocyte infiltrated area in the aortic sinus of Cont-HVJ- or mIL-10-HVJ-treated mice was shown. Macrophage infiltration was suppressed by mIL-10-HVJ treatment, whereas there was no difference in the area of T-lymphocyte infiltration between mIL-10-HVJ-treated mice and Cont-HVJ-treated mice. In (C) and (D), the area infiltrated by macrophage or T-lymphocyte was divided by the total plaque area and expressed by percentage. There was no significant difference in the macrophage/plaque area ratio ($27.0 \pm 5.2\%$ vs. $25.3 \pm 4.7\%$). T-lymphocyte-infiltrated area in the plaque was higher in mIL-10-HVJ-treated mice ($6.60 \pm 0.91\%$ vs. $3.48 \pm 0.75\%$). Open bars indicate the Cont-HVJ-treated group ($n = 8$) and closed bars show the mIL-10-HVJ-treated group ($n = 10$), respectively. Values are means ± S.E.M. of each group. $^*P < 0.05$ vs. Cont-HVJ-treated group.

atherosclerosis. Skeletal muscle can serve as an effective secretary platform for circulating proteins by gene transfer [20]. The present method would be easy applicable to human gene therapy, because the HVJ-liposome method is safe and repeated administration to the skeletal muscle can be done without causing undesirable side effects such as inflammation [13,21].

In the present study, IL-10 was detected in plasma during only a few days after the transfection, but such a level of IL-10 gene overexpression was sufficient to suppress atherosclerosis. We also performed immunohistochemical analysis of IL-10 in the plaque lesion, however IL-10 was hardly detectable in the lesion in both mIL-10-HVJ-treated and Cont-HVJ-treated apoE-KO mice (data not shown). Oslund et al. reported that IL-10 overexpression selectively in T-lymphocytes using the IL-2 promoter exhibited less atherosclerotic lesions compared with wild-type mice on C57BL/6J background, though plasma IL-10 did not appear to be increased [12]. The plasma levels of IL-10 induced by IL-10 gene transfer and their time course in the present study are in accordance with a report of Arai et al., who performed intraperitoneal gene transfer of human IL-10 using the HVJ-liposome method like us in a murine model of bleomycin-induced lung injury [22]. In their case, IL-10 gene transfer was performed 3 days prior to bleomycin treatment. Although an increase in plasma IL-10 levels was detected during only the first 2 days after the transfection, they found a significant reduction in the lung injury. Taken together, IL-10 might have an anti-inflammatory effect under remote control or affect the inflammation occurred in the different places, though the detail mechanisms of the effects were not fully clarified.

In the present study, IL-12 and IFN-γ mRNA levels in the spleen were significantly reduced by IL-10 gene transfer to the skeletal muscle. Further, plasma IFN-γ levels were also decreased in the mIL-10-HVJ treated mice. These data suggested that local IL-10 gene transfer to the muscle inhibited systemic Th1 differentiation pathway of T lymphocytes. Recently, Laurat et al. reported that downregulation of Th1 immune responses reduced atherosclerosis in apoE-KO mice [23]. Substantial evidence suggests that the existence of functionally polarized response by the $CD4^+$ T helper lymphocytes. Proinflammatory Th1 cells produce IFN-γ, TNF-α, IL-12, and IL-2, all of which activate macrophages and are thought to be involved in atherogenesis [24]. In contrast, Th2 cells produce IL-4 and IL-10, which promote antibody responses and inhibit several macrophage functions. Furthermore, Th1 and Th2 cytokines were reported to exert negative cross-regulatory effects with each other [8]. Thus, gene transfer of IL-10, one of the Th2 cytokine, might block Th1 polarization in Th1/Th2 balance and resulted in suppression of atherosclerosis in apoE-KO mice. Although the mechanism how local IL-10 gene transfer to the skeletal muscle induced such an effect is unclear, it is conceivable that the transient increase in plasma IL-10 levels might be enough to exert effects on the phenotypes of systemic T-lymphocytes. Generally speaking, naive T-lymphocytes differentiated after contacting the antigen presenting cells including macrophages in the lymph nodes or spleen. At least, the antigen presentations between those cells do not occur in the atherosclerotic lesions themselves. After the differentiation to mature T-lymphocytes, these cells moved to the targeted organs or lesions. Thus, changing the Th1/Th2 balance in the spleen might be efficient enough to affect the atherogenesis. Further studies are needed for this.

Although we showed that ectopic IL-10 expression during the early phase of atherosclerosis modified the Th1/Th2 balance, other mechanisms can be thought for the inhibition of atherogenesis by IL-10. IL-10 is reported to inhibit the function of antigen-presenting cell, such as macrophages

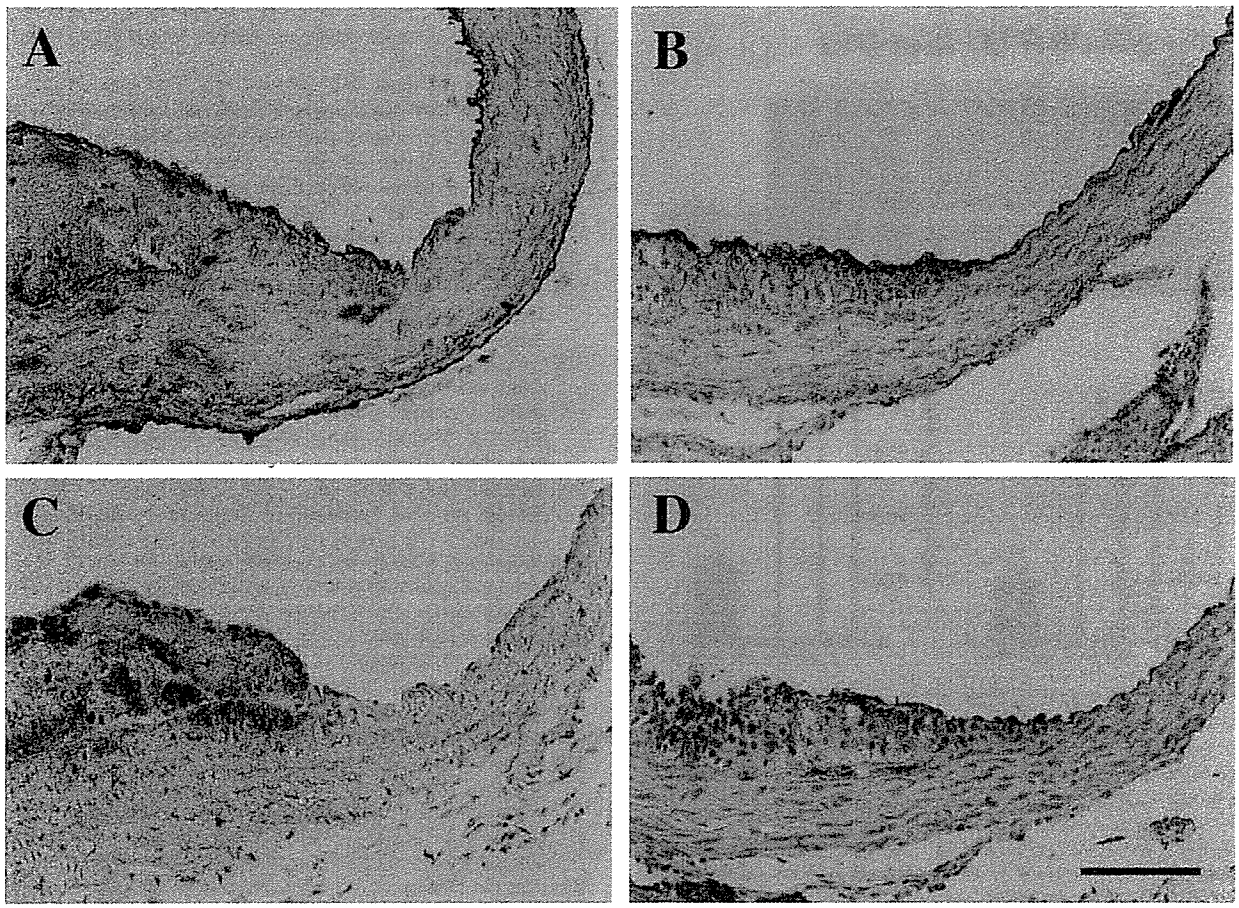

Fig. 5. Adhesion molecule expressions in atherosclerotic lesions of the ascending aorta. There were no differences in the expression of (A, B) ICAM-1 or (C, D) VCAM-1 in either plaque or non-plaque area between (A, C) Cont-HVJ-treated and (B, D) mIL-10 HVJ-treated mice. Original magnifications were ×100. A bar indicates 100 μm.

and dendric cells [4,5]. IL-10 may inhibit monocyte-endothelial interaction by suppressing the expression and/or function of adhesion molecules [25]. Adhesion of monocytes to endothelial cells plays a pivotal role in atherogenesis and monocytes constitute the main component of the plaque. Although expression of ICAM-1 or VCAM-1 at the vessel wall did not change, it is possible that IL-10 might act on monocytes and inhibited their interaction with the endothelium. Poe et al. demonstrated that IL-10 suppresses CD40-CD40 ligand-mediated monocyte responses [26], which are relevant to atherosgenesis. Therefore, inhibition of monocyte/mascrophage functions might result in suppression of atherosclerotic lesion formation [27]. On the other hand, IL-10 inhibits the production of several proinflammatory cytokines, such as IFN-γ, IL-1β, TNF-α, and IL-8 from different populations of leukocytes [28], all of which may be related to the inhibitory effects of IL-10 on atherogenesis. Clarification of the inhibitory mechanisms by IL-10 gene transfer needs to wait for future studies.

Although we demonstrated that repeated local IL-10 gene transfer inhibited atherosclerotic lesion formation in apoE-KO mice, our study may have limitations. First, we performed the first gene transfer prior to the start of the atherogenic diet. The balance between IL-12 and IL-10, that may reflect the Th1/Th2 balance, usually changes with progression of atherosclerosis. Although IL-12 can be detected both in the early atherosclerotic lesions and the progressive lesions, IL-10 is detected only in the progressive atherosclerotic lesions [8]. Therefore, the suppressive effects of IL-10 on immune response might be dependent on the stages of atherosclerosis and the timing of IL-10 treatment. Second, different from the case of mice where IL-10 preferentially regulates functions of Th1 cells, IL-10 may inhibit functions of both Th1 and Th2 cells in humans [29]. Extrapolation of our results to human atherosclerosis may need caution.

In conclusion, repeated local IL-10 gene transfer to the skeletal muscle reduced atherosclerotic lesion formation in apoE-KO mice. The inhibitory effect on atherogenesis was associated changes in the phenotype of lymphocytes. Although the anti-atherogenic mechanisms have not fully been clarified yet, IL-10 can be a therapeutic target for prevention of atherogenesis.

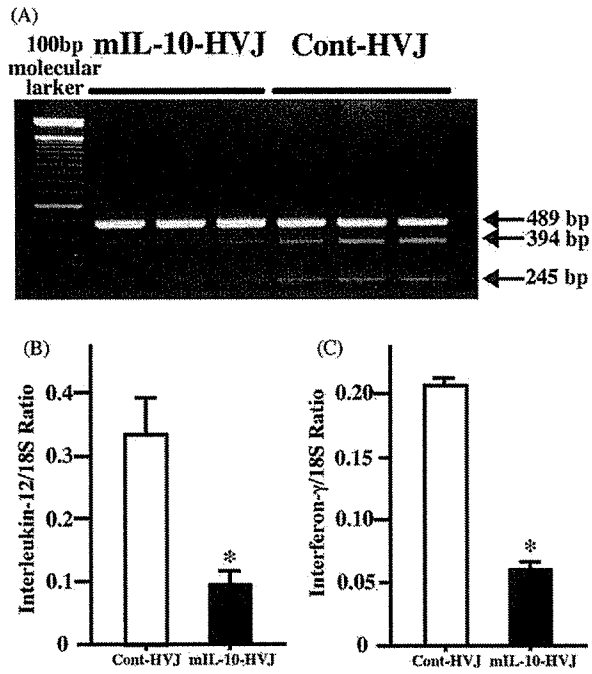

Fig. 6. Semiquantitative RT-PCR for IL-12 and IFN-γ in spleen. (A) Messenger RNA expressions of typical Th1-associated cytokine genes in the apoE-KO mouse spleen from treated with Cont-HVJ or mIL-10-HVJ. Semiquantitative RT-PCR for IL-12 and IFN-γ were performed. Treatment with mIL-10-HVJ markedly suppressed the expressions of IL-12 and IFN-γ in spleens. Lengths of the amplified fragments were 489 bp for 18S, 394 bp for IL-12 and 245 bp for IFN-γ, respectively. Band-intensity of each cytokine was measured by the densitograph software and normalized to 18S transcript as an internal control gene. Both (B) IL-12/18S ratio and (C) IFN-γ/18S ratio were suppressed by 70% in mIL-10-HVJ-treated mice compared with Cont-HVJ-treated mice ($n = 6$ in each group). Open bars indicate the Cont-HVJ-treated group and closed bars show the mIL-10-HVJ-treated group, respectively. Values are means ± S.E.M. of each group. $^*P < 0.05$ vs. Cont-HVJ-treated group.

Acknowledgements

This work was supported by Grants-in-Aid for Scientific Research on Priority Areas, Grants-in-Aid for Scientific Research from Ministry of Education, Science, Sports and Culture, Japan. We appreciate Kiyoko Matsui for their secretarial assistance and technical support for animal care.

References

[1] Ross R. Atherosclerosis-an inflammatory disease. N Engl J Med 1999;340:115–26.
[2] Apostolopoulos J, Davenport P, Tipping PG. Interleukin-8 production by macrophages from atheromatous plaques. Arterioscler Thromb Vasc Biol 1996;16:1007–12.
[3] Tedgui A, Mallat Z. Anti-inflammatory mechanisms in the vascular wall. Circ Res 2001;88:877–87.
[4] de Vries JE. Immunosuppressive and anti-inflammatory properties of interleukin 10. Ann Med 1995;27:537–41.
[5] Fiorentino DF, Zlotnik A, Mosmann TR, Howard M, O'Garra A. IL-10 inhibits cytokine production by activated macrophages. J Immunol 1991;147:3815–22.
[6] Fiorentino DF, Bond MW, Mosmann TR. Two types of mouse T helper cell. Th2 clones secrete a factor that inhibits cytokine production by Th1 clones. J Exp Med 1989;170:2081–95.
[7] Abbas AK, Murphy KM, Sher A. Functional diversity of helper T lymphocytes. Nature 1996;383:787–93.
[8] Uyemura K, Demer LL, Castle SC, Jullien D, Berliner JA, Gately MK, et al. Cross-regulatory roles of interleukin (IL)-12 and IL-10 in atherosclerosis. J Clin Invest 1996;97:2130–8.
[9] Lee TS, Yen HC, Pan CC, Chau LY. The role of interleukin 12 in the development of atherosclerosis in apoE-deficient mice. Arterioscler Thromb Vasc Biol 1999;19:734–42.
[10] Terkeltaub RA. IL-10: An immunologic scalpel for atherosclerosis? Arterioscler Thromb Vasc Biol 1999;19:2823–5.
[11] Mallat Z, Besnard S, Duriez M, Deleuze V, Emmanuel F, Bureau MF, et al. Protective role of interleukin-10 in atherosclerosis. Circ Res 1999;85:e17–24.
[12] Pinderski OLJ, Hedrick CC, Olvera T, Hagenbaugh A, Territo M, Berliner JA, et al. Interleukin-10 blocks atherosclerotic events in vitro and in vivo. Arterioscler Thromb Vasc Biol 1999;19:2847–53.
[13] Morishita R, Gibbons GH, Kaneda Y, Ogihara T, Dzau VJ. Novel in vitro gene transfer method for study of local modulators in vascular smooth muscle cells. Hypertension 1993;21:894–9.
[14] Namiki M, Kawashima S, Yamashita T, Ozaki M, Hirase T, Ishida T, et al. Overexpression of monocyte chemoattractant protein-1 at vessel wall induces infiltration of macrophages and formation of atherosclerotic lesion: synergism with hypercholesterolemia. Arterioscler Thromb Vasc Biol 2002;22:115–20.
[15] Takebe Y, Seiki M, Fujisawa J, Hoy P, Yokota K, Arai K, et al. SR alpha promoter: an efficient and versatile mammalian cDNA expression system composed of the simian virus 40 early promoter and the R-U5 segment of human T-cell leukemia virus type 1 long terminal repeat. Mol Cell Biol 1988;8:466–72.
[16] Kim JM, Brannan CI, Copeland NG, Jenkins NA, Khan TA, Moore KW. Structure of the mouse IL-10 gene and chromosomal localization of the mouse and human genes. J Immunol 1992;148:3618–23.
[17] Paigen B, Morrow A, Holmes PA, Mitchell D, Williams RA. Quantitative assessment of atherosclerotic lesions in mice. Atherosclerosis 1987;68:231–40.
[18] Yla-Herttuala S, Lipton BA, Rosenfeld ME, Sarkioja T, Yoshimura T, Leonard EJ, et al. Expression of monocyte chemoattractant protein 1 in macrophage-rich areas of human and rabbit atherosclerotic lesions. Proc Natl Acad Sci USA 1991;88:5252–6.
[19] von der Thüsen JH, Kuiper J, Fekkes ML, de Vos P, van Berkel TJC, Biessen EAL. Attenuation of atherogenesis by systemic and local adenovirus-mediated gene transfer of interleukin-10 in LDLr−/− mice. FASEB J 2001;15:2730–2.
[20] Prud'homme GJ, Lawson BR, Chang Y, Theofilopoulos AN. Immunotherapeutic gene transfer into muscle. Trends Immunol 2001;22:149–55.
[21] Tsuboniwa N, Morishita R, Hirano T, Fujimoto J, Furukawa S, Kikumori M, et al. Safety evaluation of hemagglutinating virus of Japan-artificial viral envelope liposomes in nonhuman primates. Hum Gene Ther 2001;20:469–87.
[22] Arai T, Abe K, Matsuoka H, Yoshida M, Mori M, Goya S, et al. Introduction of the interleukin-10 gene into mice inhibited bleomycin-induced lung injury in vivo. Am J Physiol 2000;278:L914–922.
[23] Laurat E, Poirier B, Tupin E, Caligiuri G, Hansson GK, Bariety J, et al. In vivo downregulation of T helper cell 1 immune responses reduces atherogenesis in apolipoprotein E-knockout mice. Circulation 2001;104:197–202.
[24] Zhou X, Paulsson G, Stemme S, Hansson GK. Hypercholesterolemia is associated with a T helper (Th) 1/Th2 switch of the autoimmune response in atherosclerotic apoE-knockout mice. J Clin Invest 1998;101:1717–25.

[25] Hickey MJ, Issekutz AC, Reinhardt PH, Fedorak RN, Kubes P. Endogenous interleukin-10 regulates hemodynamic parameters, leukocyte-endothelial cell interactions, and microvascular permeability during endotoxemia. Circ Res 1998;83:1124–31.
[26] Poe JC, Wagner Jr DH, Miller RW, Stout RD, Suttles J. IL-4 and IL-10 modulation of CD40-mediated signaling of monocyte IL-1beta synthesis and rescue from apoptosis. J Immunol 1997;159: 846–52.
[27] Ni W, Egashira K, Kitamoto S, Kataoka C, Koyanagi M, Inoue S, et al. New anti-monocyte chemoattractant protein-1 gene therapy attenuates atherosclerosis in apolipoprotein E-knockout mice. Circulation 2001;103:2096–101.
[28] Aste-Amezaga M, Ma X, Sartori A, Trinchieri G. Molecular mechanisms of the induction of IL-12 and its inhibition by IL-10. J Immunol 1998;160:5936–44.
[29] Del Prete G, De Carli M, Almerigogna F, Giudizi MG, Biagiotti R, Romagnani S. Human IL-10 is produced by both type 1 helper (Th1) and type 2 helper (Th2) T cell clones and inhibits their antigen-specific proliferation and cytokine production. J Immunol 1993;150:353–60.

Am J Physiol Heart Circ Physiol 286: H276–H282, 2004.
First published September 11, 2003; 10.1152/ajpheart.00129.2003.

Endothelial nitric oxide synthase overexpression attenuates myocardial reperfusion injury

Steven P. Jones,[1] James J. M. Greer,[1] Aman K. Kakkar,[2] P. Derek Ware,[3] Richard H. Turnage,[3] Michael Hicks,[1] Rien van Haperen,[4] Rini de Crom,[4,5] Seinosuke Kawashima,[6] Mitsuhiro Yokoyama,[6] and David J. Lefer[1,2]

[1]Department of Molecular and Cellular Physiology, [2]Cardiology Section, Department of Medicine, and [3]Department of Surgery, Louisiana State University Health Sciences Center, Shreveport, Louisiana 71130; Departments of [4]Cell Biology and Genetics and [5]Vascular Surgery, Erasmus University Medical Center, 3000 DR Rotterdam, The Netherlands; and [6]Division of Cardiovascular and Respiratory Medicine, Department of Internal Medicine, Kobe University Graduate School of Medicine, Kobe 650-0017, Japan

Submitted 11 February 2003; accepted in final form 22 August 2003

Jones, Steven P., James J. M. Greer, Aman K. Kakkar, P. Derek Ware, Richard H. Turnage, Michael Hicks, Rien van Haperen, Rini de Crom, Seinosuke Kawashima, Mitsuhiro Yokoyama, and David J. Lefer. Endothelial nitric oxide synthase overexpression attenuates myocardial reperfusion injury. *Am J Physiol Heart Circ Physiol* 286: H276–H282, 2004. First published September 11, 2003; 10.1152/ajpheart.00129.2003.—Previous studies indicate that deficiency of endothelial nitric oxide (NO) synthase (eNOS)-derived NO exacerbates myocardial reperfusion injury. We hypothesized that overexpression of eNOS would reduce the extent of myocardial ischemia-reperfusion (MI/R) injury. We investigated two distinct strains of transgenic (TG) mice overexpressing the eNOS gene (eNOS TG). Bovine eNOS was overexpressed in one strain (eNOS TG-Kobe), whereas the human eNOS gene was overexpressed in the other strain (eNOS TG-RT). Non-TG (NTG) and eNOS TG mice were subjected to 30 min of coronary artery occlusion followed by 24 h of reperfusion, and the extent of myocardial infarction was determined. Myocardial infarct size was reduced by 33% in the eNOS TG-Kobe strain ($P < 0.05$ vs. NTG) and by 32% in the eNOS TG-RT strain ($P < 0.05$ vs. NTG). However, postischemic cardiac function (cardiac output, fractional shortening) was not improved in the eNOS TG-Kobe mouse at 24 h of reperfusion [P = not significant (NS) vs. NTG]. In additional studies, eNOS TG-Kobe mice were subjected to 30 min of myocardial infarction and 7 days of reperfusion. Fractional shortening and the first derivative of left ventricular pressure were measured in eNOS TG-Kobe and NTG mice, and no significant differences in contractility were observed (P = NS) between the eNOS TG mice and NTG controls. Left ventricular end-diastolic pressure was significantly ($P < 0.05$ vs. NTG) reduced in the eNOS TG-Kobe strain at 7 days of reperfusion. The cardioprotective effects of eNOS overexpression on myocardial infarct size were ablated by N^{ω}-nitro-L-arginine methyl ester (300 mg/kg) pretreatment. Thus genetic overexpression of eNOS in mice attenuates myocardial infarction after MI/R but fails to significantly protect against postischemic myocardial contractile dysfunction in mice.

myocardial infarction; cardiac dysfunction; murine model

NITRIC OXIDE (NO) is constitutively produced by the vascular endothelium by endothelial NO synthase (eNOS) and serves to protect against cardiovascular disease. NO promotes vasodilation (4, 8), regulates leukocyte-endothelial cell interactions (17), inhibits platelet adhesion and aggregation (9, 22), attenuates smooth muscle cell proliferation (7), and may modulate cardiac myocyte function (16). Since the discovery of endothelium-derived relaxing factor (EDRF) in 1980, NO has been implicated in numerous disease states as both a beneficial and a deleterious moiety. Attenuated eNOS function and reduced NO generation is a critical early event in many cardiovascular diseases (9). NO therapy utilizing physiological levels of NO is beneficial in a number of pathophysiological states including hypercholesterolemia (9), diabetes mellitus (9), and ischemia-reperfusion (I/R) injury (11, 17, 18).

A number of previous studies (3, 20, 28–30) have demonstrated that treatment with various NO-donating compounds is highly effective in the setting of myocardial I/R (MI/R) injury. NO has also recently emerged as a crucial modulator of myocardial preconditioning, and both eNOS-derived and inducible NOS (iNOS)-derived NO are thought to mediate cardioprotection during the preconditioning process (33, 36). Furthermore, MI/R injury is significantly enhanced in eNOS-deficient animals compared with wild-type controls (12). Pharmacological inhibition of NO synthesis exacerbates MI/R injury (29), whereas administration of the NO precursor L-arginine can ameliorate MI/R injury (23, 28, 32).

Recently, transgenic (TG) mice that overexpress the eNOS gene have been developed (25, 31). Previous studies of eNOS overexpression have focused primarily on shock states (35) and atherosclerosis (27, 31). While genetic overexpression of eNOS has been shown to protect against endotoxin shock (35), the effects of eNOS overexpression in the setting of hypercholesterolemia and atherogenesis are somewhat controversial at present with conflicting reports in the literature (27, 31).

In the present study, we endeavored to determine whether overexpression of eNOS could affect the severity of MI/R injury in an in vivo murine model of acute myocardial ischemia and reperfusion injury. Specifically, we sought to examine two distinct strains of eNOS TG mice and to evaluate the effects of eNOS overexpression on myocardial infarct size and postischemic myocardial contractile function.

METHODS

eNOS Transgenic Mice

Two distinct strains of eNOS TG mice were utilized in the present study. One eNOS TG mouse was developed in Kobe, Japan (eNOS

Address for reprint requests and other correspondence: D. J. Lefer, Dept. of Molecular and Cellular Physiology, LSU Health Sciences Center, 1501 Kings Highway, Shreveport, LA 71130 (E-mail: dlefer@lsuhsc.edu).

The costs of publication of this article were defrayed in part by the payment of page charges. The article must therefore be hereby marked "*advertisement*" in accordance with 18 U.S.C. Section 1734 solely to indicate this fact.

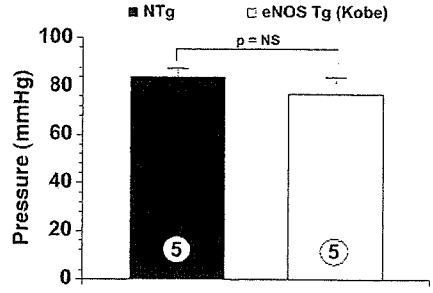

Fig. 1. Mean arterial blood pressure (in mmHg) in nontransgenic (NTG) and endothelial nitric oxide synthase (eNOS) transgenic (TG) mice developed in Kobe, Japan (eNOS TG-Kobe mice). Blood pressures were measured in anesthetized mice. No differences were observed in blood pressure between the NTG and eNOS TG mice. Numbers inside the bars are numbers of mice per group. NS, not significant.

TG-Kobe), and featured the murine prepoendothelin-1 promoter (GenBank accession no. U07982) and bovine eNOS cDNA (GenBank accession no. M99057). This mouse was developed on a C57BL/6 background and has been extensively characterized previously (15, 25–27, 34, 35).

An additional eNOS TG mouse was recently developed in Rotterdam (31), The Netherlands (eNOS TG-RT), and these mice were also used in the present study of MI/R injury. A DNA fragment containing the human eNOS gene was isolated from a homemade human genomic cosmid library (10) using eNOS cDNA (kindly donated by Dr. S. Janssens, Leuven, Belgium) as a probe (31). In addition, the DNA fragment contained ~6 kb of the 5′ natural flanking sequence, including the native eNOS promoter, and ~3 kb of the 3′ sequence to the gene. Thus promoter DNA elements were included that have been shown to be essential in transcriptional regulation as well as elements responsible for the tissue distribution of eNOS expression (19). Also, the endothelium enhancer element that is located 4.9 kb upstream from the transcription start site of the eNOS gene is included in this construct. Vector sequences were removed by restriction endonucleases. A solution of 1–2 μg/ml DNA was used for microinjection of fertilized oocytes from FVB donor mice and transplanted into the oviducts of pseudopregnant B10xCBA mice. Founder mice and offspring were genotyped by PCR on DNA isolated from tail biopsies. The primers used were as follows: 5′-GTCCTGCAGACCGTGCAGC-3′ (sense) and 5′-GGCTGTTGGTGTCTGAGCCG-3′ (antisense). Mice were backcrossed to C57BL/6 mice for at least seven generations (~99% C57BL/6). The individual performing all experiments was blinded to the mouse genotype until all data were fully analyzed. All experiments performed at Louisiana State University Health Sciences Center conformed to state and federal regulations regarding animal experimentation and with American Physiological Society guidelines.

Myocardial Infarction Protocol

Ligation of the left main coronary artery was performed similar to methods described previously (12, 14). Briefly, mice were anesthetized with intraperitoneal injections of ketamine (50 mg/kg) and pentobarbital sodium (50 mg/kg). The animals were then attached to a surgical board with their ventral side up. The mice were orally intubated with polyethylene (PE)-90 tubing connected to PE-240 tubing and then connected to a model 683 rodent ventilator (Harvard Apparatus; Natick, MA). The tidal volume was set at 2.2 ml, and the respiratory rate was set at 122 breaths/min. The mice were supplemented with 100% oxygen via the ventilator side port. A median sternotomy was performed using an electric cautery, and the proximal left main coronary artery was visualized and completely ligated with 7-0 silk suture mounted on a tapered needle (BV-1, Ethicon).

In additional experiments, both non-TG (NTG) and eNOS TG mice (eNOS TG-Kobe) were subjected to coronary artery ligation for 30 min and 24 h of reperfusion. All of the mice were treated with 5-hydroxydecanoic acid (5-HD) at a dose of 10 mg/kg 30 min before the left main coronary artery ligation (24). An additional group of eNOS TG-Kobe mice (n = 7) were treated with 300 mg/kg N^{ω}-nitro-L-arginine methyl ester (L-NAME; intraperitoneal injection) 30 min before the left main coronary artery ligation. The mice receiving L-NAME were subjected to 30 min of left main coronary artery ligation and 24 h of reperfusion. Additional experiments were also performed in C57BL/6 mice (n = 6 mice/group) treated with the NO donor dipropylenetriamine (DPTA) NONOate (Alexis Pharmaceuticals; San Diego, CA). In these experiments, mice were subjected to 30 min of myocardial ischemia and 24 h of reperfusion. DPTA NONOate (100 μg/kg) was administered 5 min before coronary artery reperfusion via direct injection into the left ventricular (LV) cavity.

Myocardial Infarct Size Determination

At 24 h of reperfusion, the mice were anesthetized as described previously, intubated, and connected to a rodent ventilator. A catheter (PE-10 tubing) was placed in the common carotid artery to allow for Evans blue dye injection. A median sternotomy was performed, and the left main coronary artery was religated in the same location as before. Evans blue dye (1.2 ml of a 2% solution) was injected into the carotid artery catheter into the heart to delineate the ischemic zone from the nonischemic zone. The heart was rapidly excised and serially sectioned along the long axis in 1-mm-thick sections, which were then incubated in 1.0% 2,3,5-triphenyltetrazolium chloride for 5 min at 37°C to demarcate the viable and nonviable myocardium within the risk zone. Each of the five 1-mm-thick myocardial slices was weighed, and the areas of infarction, risk, and nonischemic LV were assessed by a blinded observer using computer-assisted planimetry (NIH Image 1.57). All of the procedures for area at risk (AAR) and infarct size determination have been previously described (12, 14).

Evaluation of Arterial and LV Hemodynamics

At 7 days after myocardial ischemia and reperfusion, a 1.4-Fr Millar (SPR-671; Houston, TX) pressure transduction catheter was inserted similar to methods described previously (21). Data for each animal were calculated from at least 10 s of chart recording (arithmetic mean of at least 50 cardiac cycles).

Echocardiographic Assessment of LV Function

Transthoracic echocardiography of the LV using a 15-MHz linear array transducer (15L8) interfaced with a Sequoia C256 (Acuson) was performed in groups of mice after either 24 h or 7 days of reperfusion after 30 min of left main coronary artery ligation. Two-dimensional

Table 1. *Baseline cardiac function in the Kobe NTG and Kobe eNOS TG mice*

Group	Heart Rate, beats/min	Stroke Volume, μl	Cardiac Output, μl/min	LVEDD, mm	LVESD, mm	FS, %
NTG	340±18	37.9±1.6	605±20	3.54±0.13	2.64±0.11	26.7±0.3
eNOS TG	333±10	−34.6±2.6	540±33	3.56±0.10	2.50±0.10	29.9±1.8

Values are means ± SE; n = 10–11 Kobe nontransgenic (NTG) and endothelial nitric oxide synthase (eNOS) transgenic (TG) mice. LVEDD and LVESD, left ventricular end-diastolic and end-systolic diameter, respectively; FS, fractional shortening.

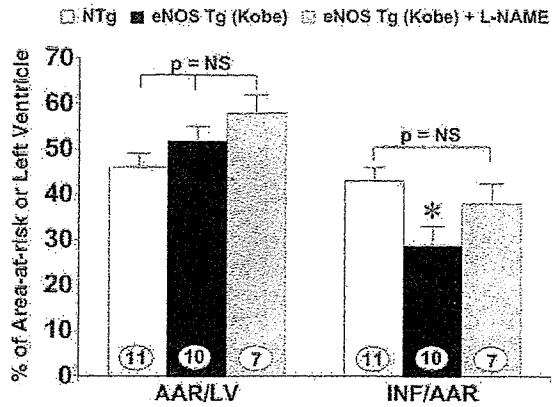

Fig. 2. Area at risk (AAR) per left ventricle (LV) and infarction (INF) per AAR in NTG and eNOS TG-Kobe mice after 30 min of coronary artery ligation and 24 h of reperfusion. The AAR was determined using Evans blue dye injection, and the infarction area was determined using 2,3,5-triphenyltetrazolium chloride staining. Myocardial infarction (MI) was significantly (*$P <$ 0.05 vs. NTG) reduced in the eNOS TG-Kobe mouse. Numbers inside the bars are numbers of mice per group. L-NAME, N^{ω}-nitro-L-arginine methyl ester.

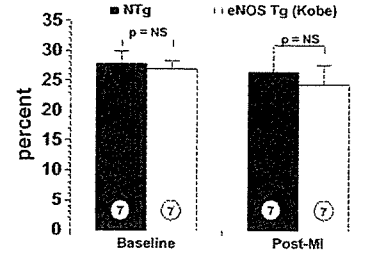

Fig. 3. Fractional shortening (in %) as measured using two-dimensional echocardiography in NTG and eNOS TG-Kobe mice after 30 min of coronary artery occlusion and 7 days of reperfusion. No significant differences were observed between the NTG and eNOS TG-Kobe groups. Numbers inside the bars are numbers of mice per group.

echocardiography was performed as described previously (13, 14). All data were calculated from 10 cardiac cycles/experiment.

Statistical Analyses

Data were analyzed by two-way ANOVA with post hoc analysis using StatView software (version 5.0, SAS Institute; Cary, NC). The Bonferroni test was used for post hoc analysis. Data are reported as means ± SE with differences accepted as significant when $P < 0.05$.

RESULTS

eNOS TG-Kobe Mice

Hemodynamics. Mean arterial blood pressure (Fig. 1) was measured in the eNOS TG-Kobe mice and NTG control animals. Blood pressure was 84 ± 4 mmHg in the NTG group and 77 ± 7 mmHg in the eNOS TG group [P = not significant (NS)]. Similarly, baseline heart rates (Table 1) were similar in the NTG (340 ± 18 beats/min) and eNOS TG (333 ± 10 beats/min) groups.

Myocardial infarct size. Myocardial AAR per LV and infarct size per AAR data after 30 min of left main coronary artery occlusion and 24 h of reperfusion are presented for NTG controls (n = 11) and eNOS TG mice (n = 10) in Fig. 2. The AARs per LV were similar (P = NS) in the NTG and eNOS TG-Kobe mice (46 ± 3% and 52 ± 3%, respectively). Myocardial infarct size per AAR was 43 ± 3% in the NTG group and 29 ± 4% in the eNOS TG group ($P > 0.05$ between the groups). In eNOS TG mice treated with L-NAME (n = 7) before myocardial ischemia, the AAR per LV was 58 ± 4% (P = NS compared with NTG and eNOS TG alone), and the myocardial infarct size per AAR was 37 ± 4% (P = NS compared with the NTG group and $P < 0.05$ compared with the eNOS TG group). In additional experiments, we investigated the effects of L-NAME treatment of eNOS TG mice at dosages of 50 and 100 mg/kg and failed to observe any changes in myocardial infarct size compared with vehicle (data not shown).

Baseline and postischemic cardiac function after 30-min myocardial infarction and 24 h of reperfusion. Baseline and postischemic cardiac function data are presented in Tables 1 and 2. No group differences in heart rate, stroke volume, cardiac output, LV end-diastolic diameter, LV end-systolic diameter, or fractional shortening were observed at baseline. After myocardial ischemia and reperfusion, the heart rate was significantly ($P < 0.05$) reduced in both the NTG and eNOS TG groups compared with baseline values. Furthermore, stroke volume and fractional shortening were also significantly ($P <$ 0.05 vs. baseline) depressed in the NTG and eNOS TG groups after 30 min of myocardial ischemia and 24 h of reperfusion.

Baseline and postischemic cardiac function after 30-min myocardial infarction and 7 days of reperfusion. An additional group of eNOS TG-Kobe mice was subjected to myocardial ischemia for 30 min followed by 7 days of reperfusion, and cardiac function was assessed. LV fractional shortening data (two-dimensional echocardiography) are presented in Fig. 3. Baseline fractional shortening was 28 ± 2% in NTG mice and 27 ± 1% in eNOS TG mice (P = NS). After MI/R, fractional shortening was 27 ± 3% in the NTG group and 24 ± 3% in the eNOS TG group (P = NS). Additional data for LV pressures (LV Millar catheter) are presented in Figs. 4 and 5 after myocardial infarction and 7 days of reperfusion. LV end-systolic pressure was 90 ± 2 mmHg in the NTG group and 85 ± 9 mmHg in the eNOS TG group (P = NS). LV end-diastolic pressures were 16 ± 6 mmHg in the NTG group and 3 ± 2 in the eNOS TG group ($P < 0.05$). LV developed pressure was 74 ± 5 mmHg in the NTG mice and 82 ± 9 in the eNOS TG mice (P = NS).

Data for the first derivative of LV pressure (LV dP/dt) are presented in Fig. 5. Positive dP/dt was similar (P = NS) in the

Table 2. *Cardiac function in Kobe NTG and Kobe eNOS TG mice after myocardial ischemia and 24 h of reperfusion*

Group	Heart Rate, beats/min	Stroke Volume, μl	Cardiac Output, μl/min	LVEDD, mm	LVESD, mm	FS, %
NTG	463±13*	23.1±2.0*	567±60	3.33±0.05	2.63±0.14	21.4±1.6*
eNOS TG	470±16*	23.7±2.9*	538±38	3.47±0.09	2.79±0.08	19.7±2.4*

Values are means ± SE; n = 10–11 mice/group. *$P < 0.05$ vs. baseline.

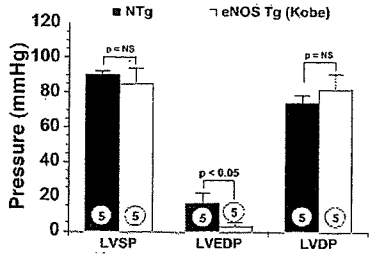

Fig. 4. LV end-systolic pressure (LVSP), LV end-diastolic (LVEDP), and LV developed pressure (LVDP) as measured using a 1.4-Fr Millar catheter placed in the LV cavity. Data were collected in NTG and eNOS TG-Kobe mice after 30 min of coronary artery occlusion and 7 days of reperfusion. No significant differences in LVSP or LVDP were observed between the groups. LVEDP was significantly ($P < 0.05$) lower in the eNOS TG-Kobe mice. Numbers inside the bars are numbers of mice per group.

NTG and eNOS TG groups (4,675 ± 1,195 and 6,300 ± 1,980 mmHg/s, respectively). Negative dP/d*t* was −3,750 ± 992 mmHg/s in the NTG animals and −6,700 ± 2,215 mmHg/s in the eNOS TG-Kobe animals (P = NS).

eNOS TG-RT Mice

Myocardial ischemia-reperfusion. Myocardial ischemia (30 min) and reperfusion (24 h) experiments were also performed in the eNOS TG-RT mouse strain. The results of these experiments are presented in Figs. 6 and 7. Mean arterial blood pressure data are shown in Fig. 6. Baseline blood pressure was 86 ± 5 mmHg in the NTG mice and 80 ± 3 mmHg in the eNOS TG mice (P = NS). The blood pressure during ischemia was reduced to 59 ± 5 mmHg in the NTG group and to 55 ± 3 mmHg in the eNOS TG group ($P < 0.05$ vs. baseline for both groups; P = NS between groups). After reperfusion, mean arterial blood pressure remained significantly depressed in both groups ($P < 0.05$ vs. baseline).

Myocardial infarct data for the eNOS TG-RT mice are presented in Fig. 7. The AAR per LV was 51 ± 4% in the NTG controls and 48 ± 7% in the eNOS TG group (P = NS). Myocardial infarct size per AAR was significantly ($P < 0.05$) reduced in the eNOS TG group (34 ± 3%) compared with the NTG group (50 ± 7%).

eNOS TG-Kobe Mice with 5-HD Treatment

Myocardial infarct size. The effects of the mitochondrial ATP-sensitive K^+ (K_{ATP}) channel blocker 5-HD on myocardial infarct size in NTG mice and the eNOS TG-Kobe strain of mice are presented in Fig. 8. Treatment with 5-HD failed to attenuate myocardial infarct size in both the eNOS TG group (P = NS vs. no treatment) and the NTG group (P = NS vs. no treatment).

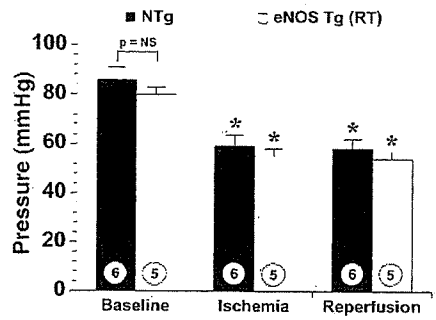

Fig. 6. Mean arterial blood pressure (in mmHg) measured in NTG and eNOS TG mice from Rotterdam, The Netherlands (eNOS TG-RT mice), at baseline and during ischemia and reperfusion. Blood pressure was measured in anesthetized mice. Blood pressure was measured at 25 min of ischemia and also at 2 h after reperfusion. Numbers inside the bars are numbers of mice per group. *$P < 0.05$ vs. baseline.

Wild-Type Mice with NO Donor Therapy

Myocardial infarct size. The effects of NO donor therapy (DPTA NONOate) were evaluated in NTG wild-type mice (n = 6 mice/group), and these data are presented in Fig. 9. The AAR per LV was 61 ± 4% in untreated wild-type mice and 63 ± 4% in wild-type mice treated with DPTA (P = NS between groups). Infarct size per AAR was 45 ± 3% in wild-type controls and 21 ± 2% in mice treated with DPTA ($P < 0.01$ between groups).

DISCUSSION

Data from the present study provide evidence for a beneficial role of genetic overexpression of eNOS in the setting of MI/R injury. Myocardial infarct size was reduced by ~33% in two distinct strains of eNOS TG mice. The bovine eNOS gene was overexpressed in one mouse strain, whereas the human eNOS gene was overexpressed in the other mouse strain. eNOS genetic expression varied from ~6- to 12-fold in these TG mice, and eNOS protein expression was confined primarily to

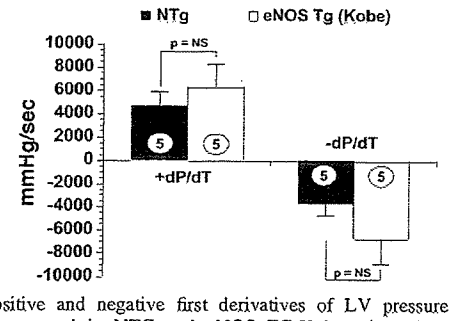

Fig. 5. Positive and negative first derivatives of LV pressure (dP/d*t*; in mmHg/s) measured in NTG and eNOS TG-Kobe mice after 30 min of coronary artery occlusion and 7 days of reperfusion. No significant group differences were observed. Numbers inside the bars are numbers of mice per group.

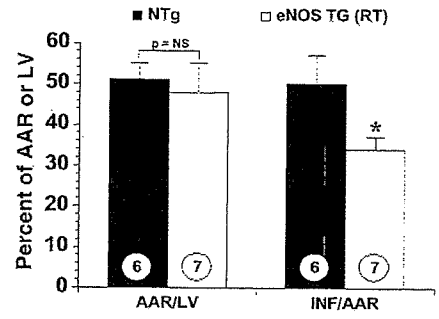

Fig. 7. Myocardial AAR per LV and infarct size per AAR in NTG and eNOS TG-RT mice after 30 min of coronary artery ischemia and 24 h of reperfusion. No significant group differences in AAR per LV were observed. Myocardial infarct size was significantly (*$P < 0.05$) reduced in eNOS TG-RT mice. Numbers within the bars are numbers of mice per group.

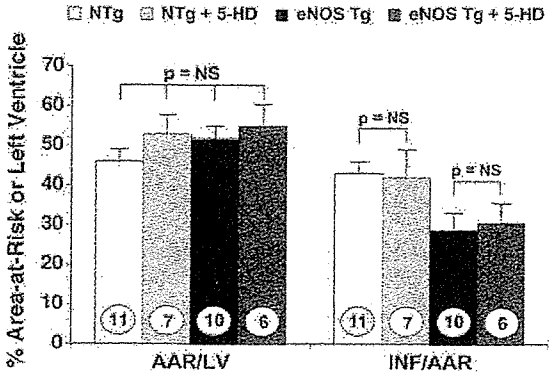

Fig. 8. Myocardial infarct size in NTG and eNOS TG-Kobe mice treated with the mitochondrial ATP-sensitive K^+ channel inhibitor 5-hydroxydecanoic acid (5-HD) at a dose of 10 mg/kg before myocardial ischemia and reperfusion. Treatment with 5-HD did not alter myocardial infarct size in the NTG or eNOS TG mice. Numbers within the bars are numbers of mice per group.

the vascular endothelium (13, 25, 27, 31). All of these improvements occurred in the eNOS TG mice without changes in systemic hemodynamics or differences in baseline ventricular morphology and function. Despite the significant reduction in myocardial infarct size, we failed to observe any significant preservation of postischemic myocardial contractile function as assessed by echocardiography or by LV direct catheterization experiments when mice were evaluated at 24 h or 7 days after myocardial infarction. It is likely that the reduction in myocardial infarct size, although significant, was not of a great enough magnitude to induce protection against postischemic contractile dysfunction. Treatment of eNOS TG mice with the NOS inhibitor L-NAME attenuated the cardioprotection observed with eNOS overexpression. These data support a cardioprotective role for eNOS in MI/R injury and further support previous studies of eNOS-deficient mice and studies of NO donors in acute MI/R injury.

Previous experimental studies of eNOS TG mice have revealed a very interesting phenotype that results from genetic overexpression of eNOS. eNOS TG mice have been shown to be protected against endotoxin shock (35) and to display systemic hypotension (25, 31). The eNOS TG mice display reduced NO-mediated vasodilator responses and appear to exhibit a nitrate tolerance (25, 34). Additionally, eNOS overexpression has been shown to limit neointimal lesion formation and medial thickening in a model of vascular remodeling (15). Overexpression of eNOS has also been shown to protect against skeletal muscle I/R injury (26). Reductions in skeletal muscle I/R injury were accompanied by a reduction in leukocyte-endothelial cell adhesion molecules and leukocyte trafficking into the ischemic tissue (26). Our laboratory has recently demonstrated (13) that genetic overexpression of eNOS significantly attenuates the severity of congestive heart failure after severe myocardial infarction in mice. Our previous study (13) clearly demonstrated significant improvements in survival and cardiac function at 30 days after myocardial infarction in the eNOS TG-RT mouse compared with NTG controls. The role of eNOS-derived NO in atherogenesis has been extensively investigated. Two strains of eNOS TG mice have been bred with apolipoprotein E-deficient mice as a means to study the potential role of NO in atherosclerosis. Interestingly, conflicting reports have emerged, with one group reporting that eNOS overexpression accelerates atherosclerotic lesion formation (27) and the other group reporting attenuated atherosclerotic lesion formation (31). Finally, both eNOS and iNOS have been selectively overexpressed within cardiac myocytes (1, 6). Cardiac myocyte-specific eNOS overexpression has been shown to blunt cardiac myofilament Ca^{2+} sensitivity without any alterations in systemic hemodynamics (1), whereas cardiac-specific iNOS overexpression did not alter cardiac function (6).

Our laboratory and others (3, 20, 23, 28–30) have previously reported that NO-donating agents significantly reduce the extent of myocardial reperfusion injury in various animal model systems. In addition, our laboratory and others have previously demonstrated that exogenous NO therapy does protect against postischemic myocardial contractile dysfunction (3, 28, 29) and that inhibition of NO promotes postischemic myocardial contractile dysfunction (5, 28). Furthermore, genetic deficiency of the eNOS enzyme significantly exacerbates MI/R injury (12). The present study provides additional support for the cardioprotective actions of NO in the setting of myocardial reperfusion injury. However, the extent of myocardial infarct size reduction observed in the present study (i.e., 32–33%) was significantly less than that reported in previous studies of exogenous NO donors (i.e., >50–65% reductions in infarct size). Furthermore, we administered the NO donor DPTA NONOate to wild-type mice in the present study and observed a highly significant 53% reduction in myocardial infarct size. One possible explanation for this apparent discrepancy is that the eNOS TG mice are exposed to elevated NO levels from the time of birth (i.e., chronic exposure), whereas NO donors have been administered to wild-type animals only for a short period of time. Thus chronic exposure to elevated eNOS and NO levels may induce myocardial tolerance, resulting in a reduction in myocardial protection compared with treatment of naïve mice with NO-donating agents. This observation may have important implications for the use of gene therapy. A previous study (34) has revealed that eNOS TG mice are resistant to NO/cGMP signaling. A recent study (2) has also demonstrated that eNOS overexpression protects isolated perfused hearts against myocardial reperfusion injury. Brunner et al. (2) demonstrated significant cardioprotection in gene-targeted mice with cardiac myocyte-specific overexpression of eNOS. Exper-

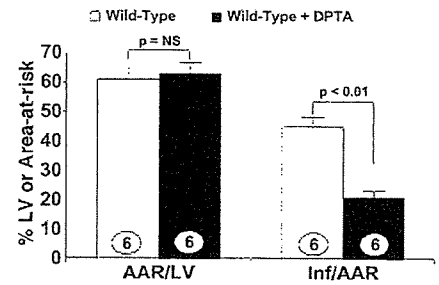

Fig. 9. Myocardial infarct size in wild-type mice treated with the NO donor dipropylenetriamine NONOate (DPTA), at a dose of 100 μg/kg 5 min before reperfusion. DPTA was injected directly into the LV. Mice were subjected to 30 min of myocardial ischemia and 24 h of reperfusion. The AAR per LV was not significantly different between groups; however, the infarct size per AAR was significantly ($P < 0.01$) attenuated in mice receiving DPTA. Numbers within the bars are numbers of mice per group.